

Available online at [www.sciencedirect.com](http://www.sciencedirect.com)

ScienceDirect

journal homepage: [www.elsevier.com/locate/AJPS](http://www.elsevier.com/locate/AJPS)

## Review

# Aspects of high-performance and bio-acceptable magnetic nanoparticles for biomedical application

Preeti Kush<sup>a</sup>, Parveen Kumar<sup>b,\*</sup>, Ranjit Singh<sup>a</sup>, Ajeet Kaushik<sup>c,\*</sup>

<sup>a</sup>School of Pharmacy, Adarsh Vijendra Institute of Pharmaceutical Sciences, Shobhit University Gangoh, Saharanpur, Uttar Pradesh 247341, India

<sup>b</sup>Nanotechnology Division (H-1), CSIR-Central Scientific Instruments Organization, Chandigarh 160030, India

<sup>c</sup>NanoBioTech Laboratory, Health System Engineering, Department of Natural Sciences, Florida Polytechnic University, Lakeland, FL 33805-8531, United States

## ARTICLE INFO

## Article history:

Received 19 March 2021

Revised 1 May 2021

Accepted 22 May 2021

Available online 4 July 2021

## Keywords:

Magnetism

Synthesis

Characterization

Delivery

Imaging

Biodistribution

Pharmacokinetic

## ABSTRACT

This review covers extensively the synthesis & surface modification, characterization, and application of magnetic nanoparticles. For biomedical applications, consideration should be given to factors such as design strategies, the synthesis process, coating, and surface passivation. The synthesis method regulates post-synthetic change and specific applications *in vitro* and *in vivo* imaging/diagnosis and pharmacotherapy/administration. Special insights have been provided on biodistribution, pharmacokinetics, and toxicity in a living system, which is imperative for their wider application in biology. These nanoparticles can be decorated with multiple contrast agents and thus can also be used as a probe for multi-mode imaging or double/triple imaging, for example, MRI-CT, MRI-PET. Similarly loading with different drug molecules/dye/fluorescent molecules and integration with other carriers have found application not only in locating these particles *in vivo* but simultaneously target drug delivery/hyperthermia inside the body. Studies are underway to collect the potential of these magnetically driven nanoparticles in various scientific fields such as particle interaction, heat conduction, imaging, and magnetism. Surely, this comprehensive data will help in the further development of advanced techniques for theranostics based on high-performance magnetic nanoparticles and will lead this research area in a new sustainable direction.

© 2021 Shenyang Pharmaceutical University. Published by Elsevier B.V.

This is an open access article under the CC BY-NC-ND license

(<http://creativecommons.org/licenses/by-nc-nd/4.0/>)

## 1. Rising of high-performance magnetic nanoparticles (HP-MNP)

In recent decades nanotechnology has successfully allowed scientists, engineers, and physicians to work together at the

cellular and molecular levels to resolve various deadlocks in science to give rise to advances in healthcare and life sciences [1,2]. Nanoparticles (NPs) size ranges up to 100 nm are widely used in biomedical and biotechnological research due to high surface area-volume ratio, high reactivity, magnified diffusion, and easy post-synthetic modification

\* Corresponding authors.

E-mail addresses: [parveenkaushik7@gmail.com](mailto:parveenkaushik7@gmail.com) (P. Kumar), [akaushik@floridapoly.edu](mailto:akaushik@floridapoly.edu) (A. Kaushik).

Peer review under responsibility of Shenyang Pharmaceutical University.  
<https://doi.org/10.1016/j.ajps.2021.05.005>

1818-0876/© 2021 Shenyang Pharmaceutical University. Published by Elsevier B.V. This is an open access article under the CC BY-NC-ND license (<http://creativecommons.org/licenses/by-nc-nd/4.0/>)

[3,4]. Among the various NPs, magnetic nanoparticles (MNPs) have demonstrated high potential applications in different research and industrial communities such as physics, chemistry, electronics, the environment, and healthcare because of remarkable new properties. These properties are superparamagnetic, additional anisotropic inputs, elevated magnetic field irreversibility, biocompatibility, non-virulence, non-immunogen, and magnetic separation [2,4-7].

MNPs play an important role as imaging agents, contrast agents, diagnostic agents, and various applications in site-specific targeting, tissue engineering, cell tracking, bioseparation, and detection of analytes [3,6,8]. For biomedical applications, various factors like design strategies, synthesis process, coating, and surface functionalization need to be considered.

MNPs are designed for site-specific delivery of therapeutic modalities in the presence of a magnetic field [4]. Thus, MNPs must exhibit high magnetic sensitivity, superparamagnetic behavior at room temperature together with dropping magnetization in the absence of a magnetic field [9]. Various types of metals (Fe, Ni, Co, Au, and Ti), ferrites, and metal oxides ( $\text{Fe}_3\text{O}_4$ ,  $\gamma\text{-Fe}_2\text{O}_3$ ) are used to prepare MNPs [3,10]. Among them, magnetite ( $\text{Fe}_3\text{O}_4$ ) and maghemite ( $\gamma\text{-Fe}_2\text{O}_3$ ) are biomaterials widely used for therapeutic applications [11,12]. Generally, pure metals need surface passivation as these are sensitive to oxidation in biological fluids even in ambient conditions [3].

MNPs are administered in a complex human biological system so these should be designed to accomplish prolong blood circulation together with magnified vascular interaction. Various physicochemical properties like particle size, surface charge, hydrophobicity, and shape should be modified for the successful transportation of MNPs through the biological membrane by escaping the immune system [1]. Regarding the evasion of the immune system, particle size plays an important role as large-sized MNPs are easily engulfed by the reticuloendothelial system (RES) and increase the possibility of vascular embolism, while the smaller particles are readily excreted [13]. Additionally, due to hydrophobicity and negatively charged surface MNPs are more prone to opsonization leading to a change in MNPs' chemical identity and making them more visible to phagocytic cells. Therefore, a wide variety of biocompatible coating materials has been used to decrease the hydrophobicity of the MNPs. Moreover, disk shape and elongated NPs exhibited magnified cellular uptake due to reduced hydrodynamic forces and increased drift velocities, compared to the spherical NPs [14]. Various synthesis methods are used for the development of MNPs with desirable properties. The synthesis method governs the post-synthetic modification and specific applications. Therefore, an appropriate methodology should be chosen to achieve the desired and specific outcome [15]. MNPs face certain limitations such as loss of magnetic property, oxidation, aggregation, and poor storage stability [16]. MNPs can be stabilized by coating using various biocompatible inorganic and organic materials like polymers, metal, metal oxides, silica, etc.

MNPs are widely used in various scientific fields, especially in biomedicine. The biomedical application includes therapeutics, diagnostics, and theragnostic applications.

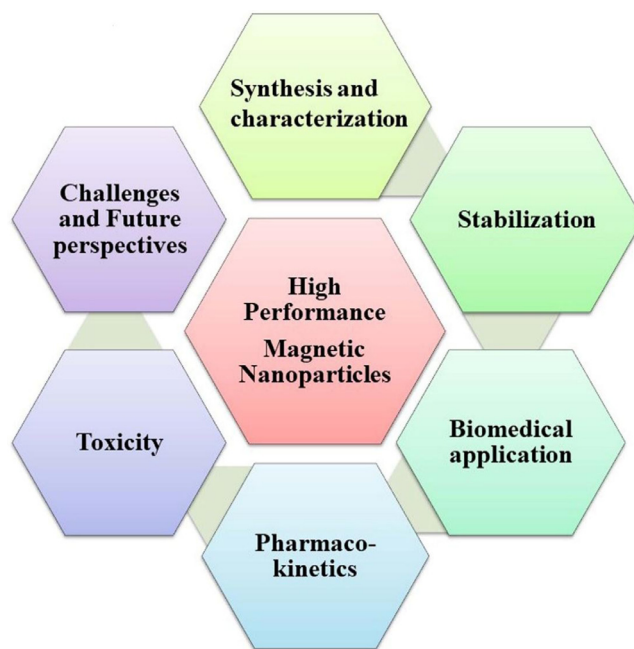


**Fig. 1 – Various aspects of high-performance MNPs.**

However, few formulations are under clinical trials/clinically used due to certain challenges like toxicity, long-term effectiveness, physiological pH stability, and specific targeting to the deeply located large blood vessels [11]. The clinical application of MNPs may be improved by post-synthetic modification of MNPs by functionalization via therapeutic modalities loading, attachment of targeting ligands/imaging molecules, and formation of nanocomposites with other biocompatible polymers or metals [17]. Post-synthetic modification is highly dependent on the specific therapeutic or diagnostic application. Additionally, functionalization also influences the pharmacokinetics and biodistribution of MNPs in biofluids [18]. In this review, efforts have been made towards the coverage of synthesis and post-synthesis modification, characterization, and further application in various fields of biology. These magnetically driven NPs have found their use in sensors, multi-mode imaging, and drug delivery. The special attraction of this work is the biodistribution & pharmacokinetic of these magnetically driven NPs. Furthermore, challenges and future aspects have also been discussed for their safer use and wider application. Fig. 1 summarizes the various aspects of high-performance and bio-acceptable MNPs for biomedical application.

## 2. Synthesis of HP-MNPs

Physical, chemical, biological, and microfluidic methods have been optimized to achieve the desired shape, size, charge, dispersion of NPs for specific applications [10,19-21]. Physical/mechanical methods including laser ablation, laser-induced pyrolysis, electron beam lithography, gas-phase deposition, are very sophisticated and give low yield. Industries need high yield methods like ball milling,

these are environment friendly and high productivity at a low cost of operations. This method is a top-down approach in which larger size particles are transformed into nano-sized particles [1,22]. Although the top-down approach is a green and inexpensive method facing certain limitations like broad particle size distribution, difficulty in functionalization, and optimization leading to limit their biological applications. Contrarily, chemical methods (also known as bottom-up or wet chemistry) involve the chemical synthesis of NPs via nucleation, growth, and condensation, which are preferred due to desired particle size, shape, and distribution. Additionally, biogenic and microfluidics methods have been extensively used for the fabrication of appropriate MNPs with desirable properties for biological applications [23]. In this section chemical and biological methods have been discussed. Table 1 summarizes the comparative analysis between various methods.

## 2.1. Chemical method

### 2.1.1. Solution precipitation

This aqueous synthesis method mainly employs three steps, nucleation, elongation or growth, and termination. Metal precursors having  $\text{Fe}^{2+}$  or  $\text{Fe}^{3+}$  individually are set to a certain temperature to obtain super saturated nuclei of these particles. Further, a precipitating agent is added which separates the elongated nuclei and continues the growth in the solution phase. The increase in the size of these particles converts the phase into precipitation and depletion of precursors results in termination. This method has been popular for decades because of its advantages such as high yield, monodispersed in size, shape uniformity, and scalability from lab to large scale. For more desirable results optimization of various process parameters like time, temperature, the concentration of various precursors involved are important. The role of surfactants can also influence the charge on the surface of these particles and hence improve the dispersion [22].

### 2.1.2. Co-precipitation methods

Co-precipitation is a simple, facile, and easy method for the synthesis of <50 nm size range MNPs by adding aqueous solutions of  $\text{Fe}^{2+}$  and  $\text{Fe}^{3+}$  ions from different precursors, in basic & anaerobic conditions at variable temperatures [4,16]. At laboratory conditions, precautions should be taken to avoid the decomposition of nanoscale magnetite ( $\text{Fe}_3\text{O}_4$ ) to maghemite ( $\text{Fe}_2\text{O}_3$ ) when dissolved in an acidic solution. In an acidic medium, the magnetite phase can be supplemented with more  $\text{Fe}^{3+}$  in the form of ferric nitrate to avoid chemical instability. There are certain parameters like  $\text{Fe}^{2+}/\text{Fe}^{3+}$  ratio, pH, temperature, surfactants, and ionic strength that need to be optimized to control the particle size, shape, and magnetic behavior of MNPs [24,25]. Despite high yield and efficient production, MNPs synthesized by this process possess irregular shapes and wide size distribution [4].

### 2.1.3. Thermal decomposition

This method is very diverse and yields monodispersed MNPs together with controlled particle size, shape, and high crystallinity. In this approach, organometallic precursors ( $\text{M}^x$

**Table 1 – Comparative analysis between the physical, chemical, biological, and microfluidics methods for the preparation of MNPs [1].**

Synthesis process	Properties									
	Yield	Reproducibility	Scalability	Stability	Operational safety	Particle size	Size distribution	Surface area/volume ratio	Optimization	
Physical	Very high	Fair	Very good	-	Poor	Small	Very wide	Small	Very poor	
Chemical	High	Poor	Good	Very good	Good	Small	Wide	Small	Good	
Biological	Low	Poor	Very good	Poor	Very good	Very small	Very narrow	High	Poor	
Microfluidics	High	Fair	Poor	Good	Very good	Very small	Narrow	High	Very good	

(N-nitroso phenylhydroxylamine)<sub>x</sub>; [M<sup>n+</sup>(acetylacetonate)<sub>n</sub>], where M is Ni, Mn, Co, Fe, Cr; n corresponds to 2 or 3; or carboxyls (such as Fe(CO)<sub>5</sub> or Fe(Cup)<sub>3</sub>) are dissolved in organic solvents along with stabilizers (oleic acid, hexadecyl amine, 1-octodecimo) and heat-treated at high temperature under anaerobic conditions for the certain time [4,26,27]. The stabilizer slows down the nucleation process leading to the formation of spherical NPs with an average size <30 nm. However, certain safety issues arise if the reaction is performed under anaerobic conditions due to the high temperature and pressure of the organic solvents and vapors. To overcome the mentioned limitation, in an anaerobic reaction Teflon-lined sealed autoclaves are used to synthesize metal oxide NPs. In this reaction ferrous hydroxide is formed in the first step which is oxidized by protons of water to iron oxide in the second step. The morphology and size of NPs can be remarkably influenced by different processing variables such as reaction time and temperature [28]. It has also been observed that annealing at various temperature and time influence the size, size distribution, dispersion, structural motifs, and magnetic properties [29]. The synthesis of these NPs in organic solutions restricts their application in biology and medicine. Even surface modification or cap exchange did not significantly affect solubility in aqueous solutions [4].

#### 2.1.4. Microwave-assisted

Microwaves are 1–1000 mm wavelength (frequency range 0.3–300 GHz) radiations which can accelerate the synthesis of NPs in reaction medium by increasing temperature. These radiations can be used solely or in combination with other methods that can interfere with the reaction scheme [30]. Generally, thermal decomposition is combined with microwave technique for synthesis and hence called a non-hydrolytic approach. However, microwaves can also assist in hydrothermal and sol-gel methods. Polar or charged ions absorb and interact with microwaves at the molecular level, resulting in the generation of heat. Microwaves are rapid in heat conversion and fasten the processing with a high reaction rate. It has been observed that this reduces the reaction time and increases the yield of the iron oxide NPs (IONPs) in a cost and energy-efficient manner [1].

#### 2.1.5. Sol-Gel

The sol-gel method comprises hydroxylation and condensation of metallic precursors in solution producing the sol-form of the NPs. Condensation and inorganic polymerization further lead to the gel form of the three-dimensional metal oxide network [10]. Initially, the reaction is carried out at room temperature but later on crystals are formed after heat treatment at a certain temperature. The size and surface morphology of the MNPs are influenced by various processing variables like the concentration and nature of metallic precursors, pH, and temperature.

#### 2.1.6. Polyol method

The polyol method facilitates the synthesis of MNPs in a liquid phase under higher boiling conditions [27]. The synthesis method is based on the oxidative alkaline hydrolysis of

metallic precursors (Fe<sup>2+</sup>, Fe<sup>3+</sup>) in a mixture of polyols (ethylene glycol, diethylene glycol, triethylene glycol, tetra ethylene glycol, polyethylene glycol (PEG), propanediol, butanediol, pentanediol, glycerol, pentaerythritol, and certain carbohydrates) [10,31]. High-temperature conditions can be achieved by conventional heating, microwave, or ultrasonication. The extra unbound polyols can be easily removed by thermal annealing, washing with water, and coordination exchangers like carboxylates, amines, etc. [32]. The particle size and shape of the MNPs can be easily optimized by varying the solvent and reaction conditions. The synthesized MNPs exhibit uniform particle size distribution, and dispersion, specifically used in magnetic resonance imaging (MRI) due to the presence of the hydroxyl group [2].

#### 2.1.7. Microemulsion method

Microemulsions or nanoreactors are thermodynamically stable isotropic dispersion of two immiscible phases (polar and non-polar) mixed in the presence of amphiphilic surfactant molecules [33]. The polar phase comprises an aqueous solution of metallic precursors and the non-polar phase usually comprises oils/mixtures of hydrocarbons and olefins. The monolayer of hydrophilic heads and hydrophobic tails of surfactants stabilize the aqueous and oil phase, respectively by lowering the surface tension between the water/oil interface. Microemulsion formation is assisted by vortexing, sonication, stirring, and homogenization. This method is more advantageous than the other synthetic approaches as the variables like speed, time, temperature, the ratio of water: oil: surfactant can be optimized to yield the desired size, shape, composition, and specific surface area [34].

#### 2.1.8. Sonochemical

Cavitation is induced by acoustic ultrasound waves in a reaction medium for hydrolysis, and thermolysis of chemicals to prepare nanostructured materials under non-equilibrium conditions. The reacting bath placed into an ultrasound irradiation machine results in hot spot creation, which bears high temperatures and significantly increases the rate of hydrolysis of metal ions. For small-scale application, a piezoelectric transducer with ultrasonic titanium horn produces high-intensity cavitation into a thermostatic glass reactor. In the cavitation process, high-intensity ultrasound (20–10 MHz) radiation is applied to a mixture of reagents dissolved in a solvent. The sporadic expansion and compression of acoustic waves oscillate the particles, generate gas bubbles, and store ultrasonic energy. Further, an increase in size to a limit collapses the bubble to release the stored energy [99]. All these activities occur in a very localized environment at high temperatures (5000–25 000 K), in a short duration to obtain nanosized particles. Volatile precursors yield amorphous NPs whereas non-volatile precursors generate crystalline nanostructured. In non-volatile precursors, around 200 nm liquid phase ring is formed before collapsing the bubble which is a governing mechanism in the reaction. The collapsing bubbles create a macro stream resulting inhomogeneous mixing at the atomic or molecular level [1].

### 2.1.9. Hydrothermal and solvothermal method

This process accompanies higher temperatures (125–250 °C) and pressures (0.3–4 MPa) in at-lined stainless-steel autoclave resulting in fast nucleation and rapid growth of small-sized MNPs [4,22]. Reactions conditions, solvent nature, stoichiometry, precursor concentration, and reaction time control the morphology and size distribution of MNPs [35]. Conventional heating methods may take hours to 3–4 d in the synthesis resulting in slow kinetics. Therefore, microwave-assisted heating is adapted to overcome the limitation leading to a fast reaction in a short time, in contrast to the conventional method [4].

## 2.2. Biological method

The biological synthesis/biogenic process employs natural resources like plant extracts, bacteria, fungi for the biomineralization of the metal precursors into NPs in mild conditions. Plants comprise various reducing agents (*e.g.*, citric acid, ascorbic acid, flavones), extracellular electron shuttle, and natural enzymes (*e.g.*, reductase, dehydrogenase), which play an important role in the biological synthesis of MNPs [22]. Biologically induced mineralization (BIM), and biologically controlled mineralization (BCM) are the two different processes utilized by the bacteria for the biosynthesis of MNPs. BIM involves microbial metabolic activity by growing them on the metal surfaces followed by metabolization of the metallic precursor into the MNPs. However, the BCM approach controls the nucleation and growth of minerals in organic matrices by using Magnetotactic bacteria [1]. Fungi-mediated synthesis is an alternative green method for the biosynthesis of MNPs due to easy culture, ability to produce ample extracellular enzymes, and resistance to mutations. Although the biological synthesis method seems an environment-friendly approach yet has several limitations like yield, purity, etc. High precursor concentration adversely affects the flora and finally yield. Moreover, maintaining aseptic conditions in the culture vessel is a challenge and an important concern. Apart from these methods ball milling can also be used to synthesize such structures [Table 2](#).

---

## 3. Physicochemical and structural characterization of HP-MNPs

Various techniques are used for the physicochemical, structural, magnetic, and functional group characterization [10]. [Table 3](#) summarizes the most commonly used characterization techniques together with advantages and limitations. This comprehensive information will be enough to explain the related properties, moreover, the authors feel that the detailed description is not in the scope of this review.

---

## 4. Stabilization of HP-MNPs

Pristine MNPs are more prone to oxidation and agglomeration due to the formation of reactive oxygen species (ROS), and strong attraction between the particles respectively.

Oxidation results in loss of magnetism and agglomeration result in elimination by the RES [10]. Moreover, MNPs become structurally unstable into the biological fluids due to the interface and hydrophobic surface effect of NPs, aqueous insolubility, aggregation, and precipitation [36]. If bare MNPs are directly administered to a living organism, the aggregated form of these NPs leadings to clog the blood vessels and reduced therapeutic potential. Therefore, MNPs should be properly stabilized via surface coating by an inert and biocompatible material that provides the core material protection, enhanced water solubility, reduction in drug-associated adverse reactions, targeted drug delivery, and extend the half-life of the drug by preventing opsonization by plasma proteins [1,37]. The nature of coating material significantly influences the particle size, pharmacokinetics, and biodistribution of the MNPs inside the body. This section summarizes various strategies used for the protection and stabilization of MNPs ([Table 4](#)).

All the strategies lead to the formation of a core-shell structure, where MNPs are core and protected by shells (coating material) [38]. Moreover, the availability of functional groups facilitates post-synthetic modification for these NPs. These functionalities can be harvested for the targeting and loading of therapeutic agents. The coating process further categorized into *in situ* coatings, and post-synthetic coating. *In situ* coating is a “one spot process” where all the MNPs components and coating materials are placed in the same reaction solutions leading to form the surface-free MNPs in water. However, this method has some limitations like poor crystallinity of the MNPs and the coating material should be soluble at pH values required to accelerate MNPs formation *eg.* organic materials. On the contrary, the post-synthetic modification comprises the exterior coating of the coating material (inorganic materials) on the bare surface of MNPs via hydrophobic interaction, ligand exchange, and direct grafting [1].

### 4.1. Organic material

#### 4.1.1. Polymeric biomaterial

Polymeric materials are remarkably used for coating/surface functionalization due to their flexibility, diversity, high energy density [37]. These have been classified as conducting or non-conducting, neutral or charged, hydrophilic or amphiphilic, homopolymer or copolymer, and synthetic or natural [1,36,39,40]. Conductive polymers are usually used in physical applications like energy harvesting in batteries and supercapacitors or biosensors. The second category *i.e.*, non conducting polymers whether synthetic or natural has found extensive applications in biomedical engineering and drug delivery. Neutral polymers (dextran, PEG) protect the NPs opsonization due to the presence of hydrophilic groups like hydroxyl and ether but cannot be easily bioconjugated owing to lack of important functional groups (*eg.* -SH, -COOH, -NH<sub>2</sub>), in contrast to the charged polymer (*eg.* chitosan, polyacrylic acid). However, MNPs coated with the charged polymer, are more susceptible to opsonization due to electrostatic attraction between the MNPs. The polymeric coating (natural/synthetic) prevents the oxidation of the MNPs leading to improved blood circulation, augmented

**Table 2 – Comparative analysis of various chemical methods.**

Synthetic approach	Reaction conditions		Yield	Size distribution	Shape optimization	Synthesis	Advantages	Disadvantages	Ref.
	Temp ( °C)	Time							
Solution precipitation	20–90	Min	High	Good	Good	Simple and easy synthesis	Particle size can be easily controlled	Multiple nucleations are required to obtain the uniform nanoparticles	[2,41]
Co-precipitation	20–90	Min	High	Relatively small	Poor	Easy, facile and efficient	Mild synthesis conditions, easy post-synthetic modification, scalable production	Processing parameters need to be optimized, less reproducibility,	[1,4,190]
Thermal decomposition	100–320	Hours	High and scalable	Very small	Very good	Complex synthesis at high temperature and pressure,	smaller particle size together with high yield, adjustable magnetic properties,	Can not be used in biomedicine due to toxic solvents used for the synthesis	[1,41,191]
Microwave-assisted	160–210	Minutes	High	Narrow	Good	Simple and efficient	Simple process, high yield, water-dispersible product	Organic solvents are required for the synthesis	[1]
Flow injection	–	10 <sup>-8</sup> –10 <sup>-5</sup> S	High and scalable	Very small	Good	Complex	High, scalable, and reproducible yield	The reagents should be continuously mixed to achieve the homogeneous product	[10,192]
Electrochemical			Poor	Quite small	Poor	Simple, atmospheric condition	The size and shape of MNPs can be easily optimized	Non-reproducible	[1,10,41]
Sol-gel	<100		High and scalable	Small	Good	Simple, easy	Size and shape can be optimized by varying various parameters	Lower mechanical strength together with high permeability	[10,41]
Polyol	80–100			Small	Good		Controlled size and shape		[2,10]
Microemulsion	20–50	Hours	Low	Relatively small	Good	Complex	Uniformity in magnetism, process parameters are easy optimized	Low yield, poor crystallinity, increased solvent consumption	[1,41]
Sonochemical	20–90	Minutes	Medium	Small	Good	Very simple, atmospheric condition	Increased mixing, relatively narrow size distribution	Specific instruments like sonicators are required for the synthesis	[1,192]
Hydrothermal	180–220	Hours	Medium	Very small	Very good	Simple, high pressure	Aqueous synthesis, particle size, and shape can be optimized, continuous production	Time-consuming, synthesis at high temperature, and pressure	[1,41]

**Table 3 – Evaluation of MNP's physicochemical properties by various characterization techniques.**

Technique	Properties	Advantage	Limitation
Atomic force microscopy	Shape, size, and dispersion	Characterization in three-dimensional form	Nanoparticle exterior surface cannot be analyzed, time-consuming
Circular dichroism	Structural and conformational variations in biomolecules	Constructive method	Conformational fluctuations
Differential light scattering	Hydrodynamic size distribution	The easy and inexpensive method, Measurement can be performed in the required solvent.	Polydispersed sample size distribution is not valid
Fluorescence correlation spectroscopy	Binding kinetics and binding affinity	Increased magnification	Only used for fluorophores
Infrared spectroscopy	Structural identification	A cheap and rapid method	Less sensitive
Mass spectroscopy	Determination of molecular weight	Precise, accurate, and sensitive	Expensive,
Near-field scanning optical microscopy	Particle shape and size	The surface study, surface interaction at the nanoscale, Simultaneous fluorescence and spectroscopic measurement, Close situation analysis.	Restricted to small areas for scan, use of cantilever may damage soft samples, tip contamination, the sample size is usually small. The fluorescent signal may quench during a long sampling time.
Nuclear magnetic resonance	Structural and conformational analysis,	Constructive	A large amount of sample is required
Scanning electron microscope/Field emission electron microscope	Size and surface morphology	Size and shape can be easily determined simultaneously	The coating material is required for the sample preparation, the sample should be dry, Expensive, and sophisticated instrument
Scanning tunneling microscopy	Size and shape heterogeneity, aggregation analysis	Atomic-level measurement,	A conductive surface should be required for the sample analysis
Small-angle X-ray scattering	Size and shape, thickness	Amorphous sample can also be analyzed	Comparatively low resolution
Superconducting quantum interference devices	Magnetic property		
Surface-enhanced Raman scattering/Raman scattering/tip-enhanced Raman spectroscopy	Size, distribution of particles, and Conformational change in the structure and biochemicals, and electronic characteristic	No requirement of sample preparation, Complementary IR data, topographical information, tissue abnormalities can be easily obtained	Weak single restricted spatial resolution compared to Rayleigh scattering Small scan Area for mapping, interference in fluorescence measurement
Transmission electron microscope	Size, shape and surface morphology, aggregation analysis	Magnified resolution,	The sample should be diluted, expensive equipment
Vibrating-sample magnetometer	Magnetic behavior	Simple and inexpensive	Poor sensitivity
X-ray diffraction analysis	The structural integrity of the crystals	Non-destructive method	Only used for the large crystalline material
X-ray photoelectron spectroscopy	Chemical composition		
Zeta potential	Surface charge determination, colloidal stability	A diverse range of sample can be analyzed	The electro-osmotic effect, inaccurate measurement, need repetition

biocompatibility together with reduced leaching of the drug [1,41]. Moreover, polymeric coating imparts numerous functional groups (eg, -SH, -COOH, -NH<sub>2</sub>) onto the MNPs surface, which facilitates various diagnostic, therapeutic, and targeting ligands. Polymers can be anchored by chemical attachment/end grafting and physical adsorption/surface encapsulation (Fig. 2A and 2B). Various natural and synthetic polymers are used for coating (Table 5). Natural polymers like alginate, chitosan, dextran, and gelatin are advantageous due

to biocompatibility, and easy fabrication process, but possess non-specific drug release to the targeting site. Synthetic polymers exhibit sustained and progressive drug release for a longer period, in contrast to the natural polymer. However, polymeric-coated MNPs are prone to an acidic solution and higher temperature resulting in loss of magnetization and instability [40].

Amphiphilic polymers/block copolymers (eg, poly (maleic anhydride-alt-1-octadecene)-PEG block copolymer,

**Table 4 – Coating materials used for the stabilization of MNPs.**

Material	Advantage	Objective	Ref
Polymeric material	Magnified solubility and permeability together with increased biocompatibility	Modified drug release enabling prolong blood circulation	[10,36]
Non-polymeric material	Enhanced aqueous solubility, prevent oxidation and aggregation	Increased MRI contrast for tumor detection	[7,10,36]
Carbon	Enhanced stability, dispersivity	Catalyst	[42]
Silica	Biocompatible, optically transparent, inert, stable	Provide exceptional hydrophilicity, targeting, and diagnosis	[36]
Metal (Gold/ Silver)	augmented biocompatibility, prevent core material corrosion	tumor therapy, thermotherapy, mri	[43]

**Table 5 – Organic coating materials used for surface functionalization and coating.**

Material	Advantage	Applications	Ref
Alginate	Augmented stability and biocompatibility, antimicrobial property, enhanced mucoadhesion	Controlled drug delivery	[1,7]
Chitosan		Drug carrier, thermotherapy, ocular drug delivery	[1,193]
Dextran	Increased stability, prolong systemic circulation, targeting	MRI, tumor drug targeting	[1,7,10]
Fatty acid	Enhancement of colloidal stability	Diagnosis and targeting of the breast, cervical cancer	[10]
Folic acid	Augmented biocompatibility,		Tumor targeting
Gelatin	Biocompatible, increased cell permeability, increased drug loading	tumor therapy, thermotherapy, gene therapy	[7]
Lipids and fatty acids	augmented biocompatibility		Cancer therapy
Polyacrylic acids	Augmented bioavailability and stability	Biosensor	[7]
Polydopamine		Tumor diagnosis	[1,194]
PEG	Magnified water solubility, decreased phagocytosis, biocompatible, prolonged systemic circulation	Cell separation, hyperthermia, targeted drug delivery	[7,36]
PEI	Site-specific targeting		Cancer therapy
Poly(lactic co glycolic acid)	Magnified water solubility, decreased phagocytosis, biocompatible, prolonged systemic circulation	Drug targeting	[1]
Polymethyl methacrylate	Low cost, biocompatible		Bioseparation, MRI,
Polyvinyl alcohol	Minimize particle aggregation, enhanced stability	MRI, breast cancer therapy	[1,7,10]
Polyvinyl pyrrolidone	Increased stability, prolong systemic circulation		Imaging and sensing
Starch	Biocompatible, increased cell permeability		

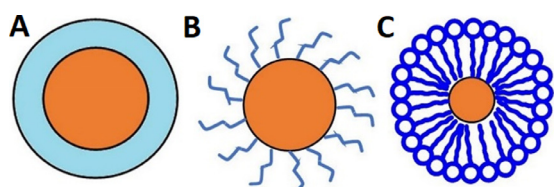


**Fig. 2 – Stabilization of MNPs via polymeric material; (A) Physical adsorption/surface encapsulation of polymer, (B) Chemical attachment/end grafting of polymer, (C) Hydrophobic interaction of amphiphilic polymers. Brown and blue colors present magnetic core and polymeric coating respectively.**

polystyrene–polyacrylic acid (PS-PAA) block copolymers) composed of lipophilic and hydrophilic components have been evolved to overcome the limitations of the single coating polymer. The lipophilic component interacts with the NPs non-polar surface via hydrophobic interaction (Fig. 2C) enabling the complete encapsulation of the core whereas, the hydrophilic part increases the aqueous solubility of the NPs enabling the bioavailability. The NPs are supposed to be stable via the shielding effect of ligand and aggregation is conquered due to the steric repulsion [36].

#### 4.1.2. Non-polymeric materials

Small organic molecules like surfactants, carboxylates, and organophosphorus molecules are commonly used for the stabilization of NPs via the formation of micelle and



liposomes [1,36]. Lipophilic surfactants such as oleic acid and oleylamine are firmly attached to the MNPs' surface via a coordination bond, which provides a protective layer enabling colloidal stability and prevents aggregation and oxidation [36]. However, biomedically these lipophilic MNPs are not effective therapeutically due to poor aqueous solubility. Various organic molecules like amino acids, vitamins, cyclodextrin, dopamine, dimercaptosuccinic acid have been used to increase the hydrophilicity of the MNPs [7].

Carboxylates like dimercaptosuccinic acids and citric acid have been commercially used for the stabilization of IONPs, through the formation of a coordination bond between the metal surface and carboxylic acid. However, this functionalization is labile to temperature due to the presence of carboxylic acid. Organophosphorous molecules such as phosphonic acid, alkyl phosphoric acid, phosphates, and phosphonates come up with stronger bonds (Fe–O–P), enabling enhanced stability at physiological pH, in contrast to carboxylates [1].

#### 4.2. Inorganic material

##### 4.2.1. Carbon

Carbon-based inorganic materials like carbon NPs, carbon dots, carbon nanotubes, graphene are also used for the surface coating of MNPs to magnify the biocompatibility, dispersivity, and stability [7,42]. These nanocomposites are mainly used as supercapacitors, catalysts, and microwave absorbers. However, research work is still in progress for therapeutic *in vitro* and *in vivo* evaluation of these nanocomposites. Recently Lee et al. demonstrated the enhanced therapeutic efficacy of carbon-coated MNPs in Zebrafish. The results stipulated that the carbon-coated MNPs are safer than the bare MNPs [42].

##### 4.2.2. Silica

Silica is a biocompatible, hydrophilic coating material used to conserve the unique properties of MNPs [7]. The core material of MNPs is electrostatically and sterically protected by the silica layer via the covalent linkage between the polymeric silica and positively charged core material [36]. Moreover, the silica-coated MNPs are optically transparent, freely dispersed in biofluids due to their negative charge at blood pH. Furthermore, this material is widely used in therapeutic, and diagnostic applications due to its extraordinary aqueous solubility, thermal resistance, high surface area, exceptional mechanical strength, and subsequent functionalization (Fig. 3A). Various techniques have been utilized for the silica coating like the Stober, microemulsion, aerosol pyrolysis, and sol–gel methods. [1,36]. However, silica coating faces certain limitations like non-biodegradability, inherent instability at basic medium, oxygen diffusivity to the magnetic core due to the porosity of the amorphous coating layer [1].

##### 4.2.3. Metals

Metals like Gold and Silver are widely used for surface coating due to their stability and compatibility, usually expressed as core–shell, dumbbell, and satellite-like structures (Fig. 3B–3D). Furthermore, the metallic inert coating layer facilitates surface functionalization enabling the targeting application of coated MNPs [7]. Gold-coated MNPs are synthesized

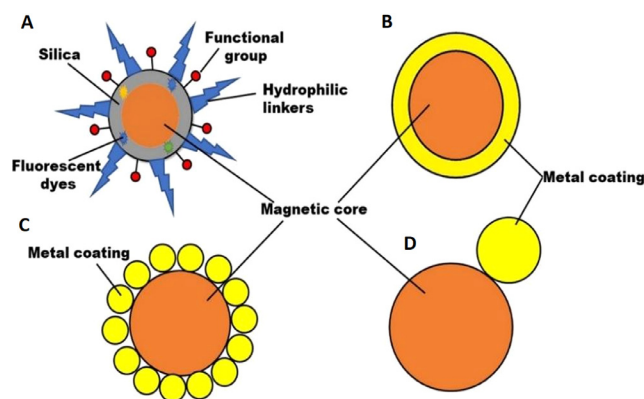


**Fig. 3 – Surface functionalization of MNPs (A) silica coating; (B) core-shell structure; (C) dumbbell and satellite-like structure.**

by microemulsion, self-assembly, chemical reduction, thermal decomposition, coprecipitation, sonochemical reaction, seed-mediated growth, and laser irradiation process [1]. Gold-coated MNPs are extensively used in enzyme immobilization, immunoassays, bioseparation, and purification, and diagnostic applications due to their unique properties [43]. Gold-coating is advantageous due to its lesser reactivity and toxicity. Additionally, gold coating retained the superparamagnetic nature of magnetic cores even after the increase or decrease in the level of magnetization [1]. Furthermore, the synergistic effect of MNPs intrinsic potential and near-infrared light sensitivity of gold-coated MNPs make them used as magnetic resonance/optical dual imaging. Altogether gold coating is advantageous but few problems should be controlled. The shell coating via the direct method is difficult due to the dissimilar nature of the two surfaces resulting in the weak coating, which can be controlled by using a linking material eg.  $\text{TiO}_2$  [1]. Silver-coated MNPs possess both optical and magnetic properties together with improved biocompatibility [43]. Silver decorated MNPs have been reported to show peroxidase and antibacterial activity. Such MNPs have also found application in biosensing of nucleic acid and *in vitro* diagnostics etc. [7].

## 5. Biomedical application of HP-MNPs

MNPs are widely used in various fields of the scientific world due to their unique properties. For biomedical applications, various components are assembled into the MNPs resulting in HP-MNPs that possess the following features (Fig. 4) [36].

1. The magnetic core is the integral and important part of the MNPs on which various components are assembled for the diagnosis and treatment of various diseases.
2. Various therapeutic modalities like drugs, genes, viruses, etc. are incorporated or surface anchored for the specific applications to the confined area.
3. MNPs are stabilized via surface coating by an inert and biocompatible material that provides core material protection and enhanced aqueous solubility.

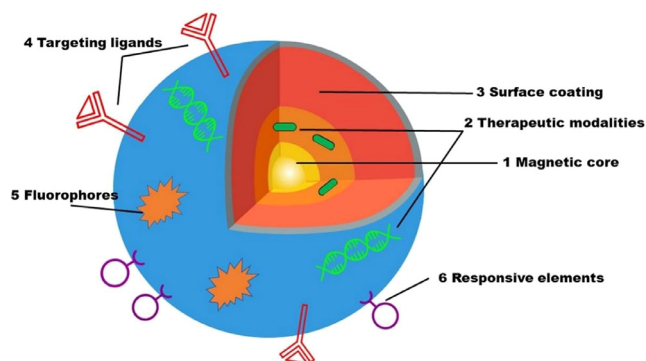


**Fig. 4 – Functionalization of various constituents on the surface of MNPs resulting in the formation of HP-MNPs for various biomedical applications.**

4. Surface anchored targeting ligands imparting the specific drug delivery to the target area by recognizing specific receptors or biomarkers.
5. Fluorophores impart imaging and diagnosis by using various diagnostic techniques.
6. Responsive elements are sensitive to different external stimuli (temperature, light) release the cargo after the stimulus.

Thus, HP-MNPs are hybrid structures comprising biocompatible polymeric/metallic shells and nanocomposites possessing diverse properties. Based on the various constituents' biomedical applications are further classified into therapeutic, and diagnostic.

### 5.1. Therapeutic application of HP-MNPs

MNPs are extensively used therapeutically due to their unique magnetic properties and biocompatibility. This section comprises various therapeutic applications of HP-MNPs together with targeting a specific area.

#### 5.1.1. Drug delivery and site-specific targeting

MNPs are widely used for the delivery of various therapeutic modalities like chemotherapeutics, immunosuppressants, antibiotics, antiviral, antifungal, anticonvulsants, anti-inflammatory, etc., owing to their large surface to volume, easy to control drug release [16,44,45]. The therapeutic modalities can be incorporated inside the matrix via adsorption, dispersion, and encapsulation or directly anchored on the MNPs surface via covalent attachment and electrostatic interaction [16]. Additionally, MNPs are also used for site-specific targeting and magnetic drug targeting (MDT) due to specific ligand attachment and superparamagnetic properties respectively enabling the reduction of the non-targeted drugs associated with adverse effects. The success of these applications depends on particle size, surface chemistry, magnetic polarization, and magnetophoretic movability under an external magnetic field (EMF) [1,3]. MNPs with size ranges of 10–100 nm are optimal for prolonged drug delivery. Particles smaller than 10 nm are easily eliminated by extravasation and renal clearance

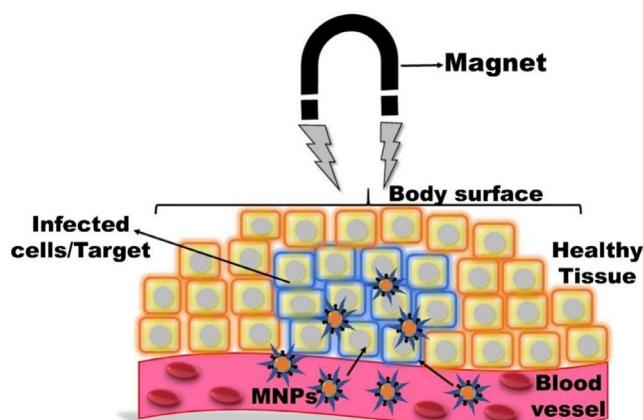


**Fig. 5 – Specific target drug delivery of MNPs under the influence of EMF.**

whereas the upper limit is not clearly defined [3]. MNPs coated with hydrophilic substances favor prolonged systemic circulation via evasion of RES. In-vivo MDT depends on the blood flow, inherent magnetic properties of MNPs, the volume of MNPs, and strength of externally applied magnetic field (EAMF) leading to accumulating the therapeutically loaded particles to the specific target (Fig. 5). However, MDT is not so effective in deep tissue targets due to less penetration of EAMF, although this can be achieved by further focusing or enhancing the magnetic field on targeted areas. MDT can show better effectiveness in nodes but again it has a poor effect on metastasis cells or tumors. It is again a concern whether the focused EAMF can adversely affect the healthy cells.

Predominantly, an external magnetic stimulus is used for the magnetic drug targeting by using external placed magnets due to safety and simplicity [46]. Various types of external magnets like permanent magnets and electromagnets are used clinically [46,47]. Permanent magnets are the cheap and widely used compact type of magnets due to their ability to produce strong EMF to a specific local area without involving a power supply and cooling system in comparison to electromagnets. However, the clinical relevancy of these magnets is hampered due to difficulty in predicting the systemic magnetic response of MNPs generated by these magnets. Furthermore, the magnetic field strength reduces with increased target length. Therefore, magnet design and orientation need to be properly addressed for effective MDT [1]. Halbach cylinder has an advantage over the permanent magnets as it focuses the magnetic field on the interior organs in a 3D manner to obtain 3D images. This dynamic control of EAMF enables a magnetic manipulator to target and guide the magnetic particles with more precision [48]. Magnetic implants are viable alternatives for deeper tissue targeting rather than an external magnet. Very few implanted magnets have been used for targeting the brain, retina, heart, and spinal cord [45]. Recently, biocompatible implanted magnets (magnetite/poly(lactic-co-glycolic acid)) exhibited superior magnetic property as compared to the EMF leading to effective bone cancer treatment [56]. In other studies, drug-

loaded MNPs were implanted inside adipose tissue and inner ear to treat obesity [57], and deafness respectively [58].

Six types of materials (eg, diamagnetic, paramagnetic, ferromagnetic, superparamagnetic, ferromagnetic, and antiferromagnetic) are used for the preparation of MNPs [22]. Among them, superparamagnetic iron oxide NPs (SPIONs) are extensively used for therapeutic application owing to high magnetic sensitivity, superparamagnetic behavior at room temperature together with dropping magnetization in the absence of a magnetic field. Moreover, SPIONs diminishes the probability of aggregation and thrombosis [1]. Al-Jamal et al. investigated the effect of SPIONs loading and strength of EAMF on mice bearing CT26 tumors. It was observed that in-vivo tumor targeting was directly proportional to SPIONs concentration and EAMF strength. Further, an *in vivo* tumor growth delay study was conducted by using a docetaxel-loaded nanocomposite. Enhanced therapeutic efficacy and improved mice survival were achieved in contrast to passive targeting of docetaxel [49].

Despite the promising results, SPIONs face some limitations like faster dissolution in-vivo and risk of cancer growth by the release of iron. Therefore, it is a prerequisite to prevent iron loss from the SPIONs by various surface coating agents like PEG, and polyvinyl alcohol (PVA-colloidal stability), natural polymers (biocompatibility), and silica (prevent iron release). Silica is the most appropriate coating material, that prevents the surface corrosion of SPIONs together with the controlled release of drugs. Recently, Recezyska et al. coated SPIONs with different silica layers (non-porous, mesoporous, both) by the sol-gel method. All these layers significantly affected the surface properties of pristine SPIONs and a nearly 10x decrease in the iron release was attained. Further in-vitro testing of these SPIONs and SPIONs@SiO<sub>2</sub> on human lung epithelial cells (A549 and BEAS-2B) proved their cytocompatibility for future applications [50].

Additionally, various diverse approaches have also been used for the development of HP-MNPs based smart material by integration of MNPs with different novel multifunctional formulations and stimuli-responsive polymers. Recently, smart materials like magnetoliposomes (MLs), magnetic microrobots [17], stimuli-responsive magnetic nanosystem [1,51], and magnetic metal-organic frameworks (MMOFs) [52,53] are the most promising carrier for the specific drug delivery together with the required dose at right time at the specific target site.

MLs are an integrated form of MNP and liposomes where MNPs are embedded into the liposomes for wide biomedical use. Szuplewska et al., fabricated doxorubicin (Dox) encapsulated MLs for the treatment of breast cancer. The magnetic properties of hydrophobic IONPs encapsulated exclusively in the lipid bilayer of liposomes were used to release Dox from the MLs. Further, the cell viability results demonstrated that the developed formulation was biocompatible and effective for the treatment of breast cancer [54]. In another study, methotrexate (MTX) loaded thermosensitive MLs were prepared for the target delivery to cervical cancer. The drug was released under the stimulation of a light/magnetic field. The tailored formulation exhibited magnificent targeting, temperature sensitivity, and highly responsive to the applied EMF. Moreover, the formulation

displayed augmented Dox uptake and release into the cell lines leading to improve cancer-killing. Hence, the tailored formulation exhibited a synergistic cytotoxic effect due to the stimuli-responsive release and MDT [55].

Microrobots are small microscopic particles that are self capable of locomotion, sensing, and have functional activities. Microrobots can be used biomedically due to various functional components like reservoirs, microactuators, and microsensors [56]. Various microrobots using MNPs have been developed for drug delivery application by surface modifications. Kim et al. proposed a novel microrobot by using gelatin/PVA-based hydrogel, MNPs, and Dox loaded poly lactic-co-glycolic acid NPs (Dox-PLGA- NPs). The fabricated hydrogel-based microrobot was targeted to a specific site via electromagnetic actuation (EMA) and followed by decomposition by near-infrared (NIR) radiation. The decomposed microrobot released MNPs, and Dox-PLGA-NPs leading to generate the therapeutic effect at the targeted area [57].

The integration of MNPs' unique properties with stimuli-responsive polymers like pH temperature, enzyme, and light, enables the control of MNPs properties operated by polymers and *vice versa*. These stimuli-sensitive magnetic nanosystems are widely used for specific target delivery of various drugs owing to their stimuli responsiveness [58]. Ghamkhari et al. fabricated a temperature and pH-sensitive magnetic nanosystem for the target delivery of Dox to tumors. The fabricated nanosystem was prepared by the adsorption of the triblock copolymer of poly[(2-succinyloxyethylmethacrylate)-b-(N-isopropyl acrylamide)-b-dimethyl-aminoethyl methacrylate) on the surface of SPIONs. The in-vitro drug release results revealed that the drug was released more effectively (53.13%) in acidic pH (5.4) in contrast to normal physiological pH (pH 7.4 and -38.04%). Similarly, the release rate was higher above the lower critical solution temperature (LCST~41–42 °C). Based on the *in vitro* drug release behavior dual responsiveness was observed leading to maintain the drug concentration at the target area. Further, the cytotoxicity results confirmed that the tailored formulation was more cytotoxic and biocompatible in contrast to native Dox [59]. Recently, an efficient ROS-sensitive sulfasalazine (SSZ) loaded magnetic nanosystem was developed for the treatment of rheumatoid arthritis (RA). The nanosystem comprises dihydro ascorbic acid (DHAA)-Fe<sub>3</sub>O<sub>4</sub>@hyaluronic acid (HA) core/shell structure containing SSZ (DHAA-Fe<sub>3</sub>O<sub>4</sub>@HA@SSZ). The drug release experiment revealed that the SSZ was released progressively in a controlled manner for a prolonged time. Further, *in vivo* studies exhibited magnified anti-inflammatory activity due to the ROS sensitivity and scavenging effect of HA. Additionally, histopathological results revealed that the tailored formulation showed magnified tissue repairing. Moreover, the radiographic images displayed that there was no sclerosis in the animals treated with DHAA-Fe<sub>3</sub>O<sub>4</sub>@HA@SSZ. In conclusion, the tailored formulation was effective for the treatment of RA without any adverse effects [60].

MMOFs are the integration of MNPs to the surface or pore of MOFs possessing the dual properties of MNPs and MOFs [61]. Hashemipour et al. prepared copper-based MMOF for

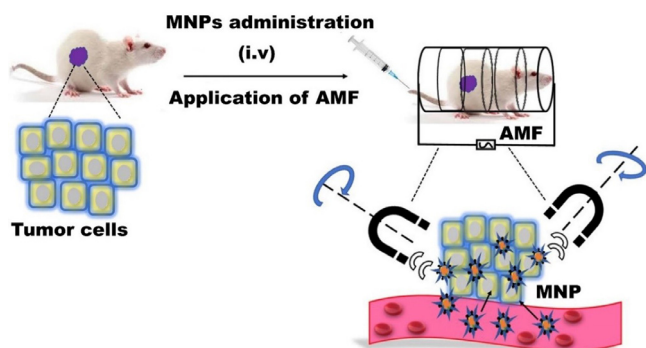


**Fig. 6 – Treatment of tumor cells using magnetic hyperthermia after i.v. administration of MNPs. The electromagnetic energy transformed into thermal energy under an AMF leading to killing the specific tumor cells.**

the sustained delivery of letrozole. The study revealed that MNPs are chemically linked with the MOFs resulting in higher loading of the drug due to the enormous surface area of MOFs. Further, in-vitro drug release data showed that the MMOFs can release the drug in the gastric and intestinal medium [62]. Another example of MMOFs is for the magnetophoretic delivery of dopamine (DA) for Parkinson's disease by Pinna et al. In this study,  $\text{Fe}_3\text{O}_4$  polymeric magnetic particles (PMPs) were encapsulated in MIL-88A (PMP@MIL-88A) and followed by encapsulation of DA into the porous PMP@MIL-88A. The tailored formulation was found biocompatible when tested on brain cancer PC12 cells using a trypan blue exclusion assay. It was observed that PMP@MIL-88A led to the increased intracellular concentration of DA whereas, decreased level in the extracellular region in contrast to native DA, hence fewer adverse effects from DA oxidation [63].

### 5.1.2. Magnetic hyperthermia

Thermotherapy is an adjuvant alternative therapy for the treatment of various cancers by using thermal energy [17,51]. Traditionally thermotherapy comprises two approaches i.e. hyperthermia and thermal ablation for the killing of tumoral cells. Hyperthermia, where the cells (normal and cancer) exhibit apoptosis under the exposure of higher temperatures range between 41 and 45 °C whereas, thermal ablation uses temperature above 45 °C leading to the necrosis of cancer cells [3,51]. Higher temperatures can be achieved by microwaves, ultrasound, and radiofrequency radiation. The success of this method is based on the higher temperature sensitivity of tumor cells than the healthy cells due to low pH and magnified glycolic activity [35,51]. However, this traditional method faces certain issues like low penetration depths and limited targeting leading to adverse effects [1].

Magnetic hyperthermia (MH) is an alternative nontoxic and non-invasive approach to overcome the above-mentioned shortcomings, where MNPs are used as heat mediators and focused the heat on the specific local area via transformation of electromagnetic energy into thermal energy by an alternating magnetic field (AMF) (Fig. 6). The intense, localized, and targeted heating selectively kills the tumor cells as a result of MNPs magnetic moment while least

affecting the neighboring healthy normal cells, which is still a limitation of chemotherapy and radiotherapy [6]. This method is superior to the traditional method owing to the localized heating of the cancer tissues or cells via easy placement of the MNPs in a deeper tumor area [1]. Moreover, MNPs can be used simultaneously as therapeutic and diagnostic agents due to their surface functionalization [35]. The transformation of oscillating electromagnetic energy into heat energy is mainly governed by three mechanisms including hysteresis loss, Brownian relaxation, and Neel relaxation [1]. The heating effect of MNPs is significantly influenced by eddy current, hysteresis effect, domain wall, relaxation effect, natural resonance, and experimental conditions (eg. frequency and strength of the AMF) [1,6,17,51]. Moreover, the magnitude of specific heat absorption rate (SAR) is dependent on the size, shape, composition, and surface chemistry of MNPs. Additionally, these factors also influence saturation magnetization ( $M_s$ ), magnetic susceptibility, relaxation time, and magnetocrystalline anisotropy ( $K$ ) [64].

Larger MNPs with a diameter >100 nm generate more hysteresis loss that governs the energy depletion by reversal magnetization. However, smaller MNPs convert to a single domain and exhibit superparamagnetic behavior with a smaller/closed hysteresis loop. Nano-MNPs exhibit magnified thermal efficiency contrarily to micrometric MNPs. Some studies revealed the importance of shape on the  $K$  factor resulting in a significant difference in MH. It was observed that nanocubes MNPs exhibited higher SAR than the spherical, despite identical composition and size [65], whereas, the chain-like magnetotactic bacteria exhibited higher heating in contrast to random [66]. The SAR can also be increased by regulating the composition of MNPs via magnetism modification. Metallic MNPs such as Fe and possess augmented SAR due to high  $M_s$  but unstable at ambient atmosphere. Further divalent transition metal cations such as  $\text{Fe}^{2+}$ ,  $\text{Co}^{2+}$ ,  $\text{Ni}^{2+}$ , and  $\text{Mn}^{2+}$  have been used to magnify the SAR. Recently, folate conjugated pegylated SPIONs were fabricated for the MH application. The fabricated SPIONs were more colloidal stable with magnified heat generation [67]. Kandasamy et al. functionalized SPIONs by various short-chain molecules such as 1,4-diaminobenzene (1,4-DAB), 3,4-aminobenzoic acid (3,4-DABA), and 4-aminobenzoic acid (4-ABA) and their combination with trimesic acid (TMA)/terephthalic acid (TA)/2-aminoterephthalic acid (ATA)/pyromellitic acid (PMA). All the surface-functionalized SPIONs showed superparamagnetic behavior but only 1,4-DAB, 3,4-DABA, 4-ABA, and 4ABA-TA-coated SPIONs exhibited excellent water dispersibility with higher  $M_s$  (~55–71 emu/g) [68].

Among the various MNPs, SPIONs are extensively used for MH due to their biocompatibility and biodegradability. Recently, Piehler et al. studied the antitumor effect of Dox-loaded IONPs on breast cancer cell lines (BT 474). They showed that the tailored formulation was more effective in contrast to single MH and native Dox due to the synergistic effect of MH and Dox [68]. However, their practical application was hampered due to poor thermal conversion efficiency. As previously discussed, the thermal conversion efficiency can be magnified by modulating MNPs size, shape, composition, and surface functionalization [64].

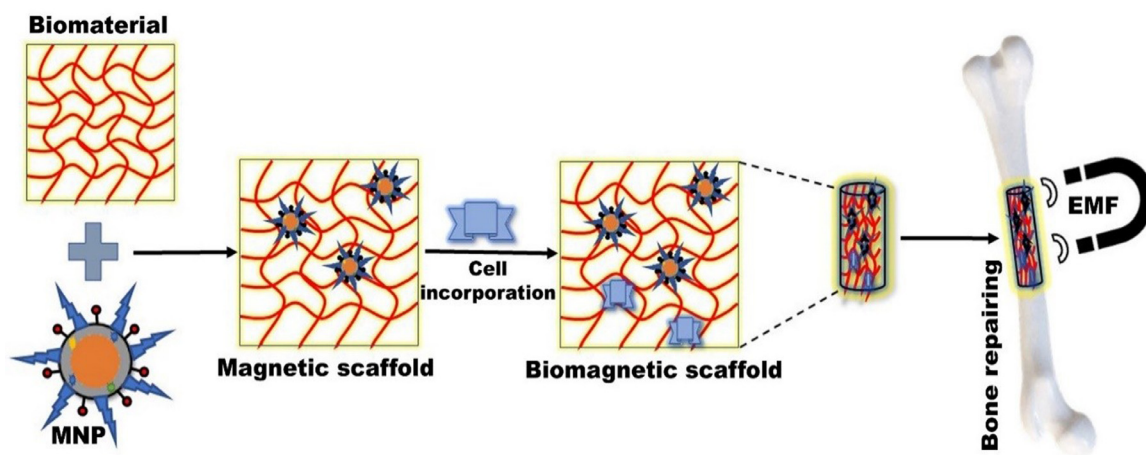


**Fig. 7 – Specific tissue engineering employing MNPs through the administration of biomagnetic scaffold (biomaterial+MNPs+desired cells) with the EMF.**

Furthermore, MNPs based MH therapy has been synergized by combining MNPs with various organic/inorganic material results in biocompatible nanocomposites with multifunctionality. As per the literature, various micro/nano composites like stimuli-responsive magnetic nano micelles [69,70], ultramagnetic liposomes [71,72], graphene oxide (GO)-IONPs [73,74], magnetic mesoporous silica NPs [75,76], and MMOFs, etc. [77] have been developed for synergistic MH therapy and drug delivery. Recently, a study showed that IONPs grafted on GO surface with Dox were more effective and safe for drug delivery and MH therapy [78]. In another study, Asgari et al. showed the enhanced therapeutic efficacy of silica-coated curcumin-loaded IONPs for the controlled drug delivery and MH therapy. The tailored formulation exhibited pH-responsive release and enhanced cytotoxicity due to the silica coating [75]. Recently, Chen et al. developed a Dox-loaded MMOF ( $\text{Fe}_3\text{O}_4\text{@PDA@ZIF-90}$ ) by the surface coating of zeolitic imidazolate frameworks (ZIFs) on the surface of polydopamine (PDA) coated iron NPs for synergistic MH. The tailored nanocomposite exhibited superior loading capacity with pH-responsive drug release. Further, the nanocomposite raised the local temperature from 30 to 77.5 °C-under AMF due to the magnetocaloric effect of iron cores [77]. Biominerallized bacterial MNPs are another alternative approach to enhance the MH effect. Gandia et al. showed that the biological structure of magnetotactic bacteria (*Magnetospirillum gryphiswaldense*) exhibited superior hyperthermia without disturbing cell proliferation [79].

### 5.1.3. Tissue engineering

Tissue engineering (TE) employing MNPs has achieved either fusing i.e., connecting two surfaces, and followed by joining the tissues via heating or soldering [80], where MNPs are integrated with other biocompatible material leading to form a magnetic scaffold [51]. The scaffold loaded with desired cells (mesenchymal stem cells, natural killer cells erythrocytes), protein, growth factors, and tissues are administered and focused on the specific tissues by using EMF (Fig. 7) [3].

These scaffolds control and support the cellular responses via targeting specific cellular receptors and have found application in tissue repairs like bone, muscles, nerves, and disease treatment [80]. In the biomagnetic approach, MNPs present on/in the cells and magnetic scaffold may interact with each other under dynamic/static remote EMF to control spatial and/or temporal precision to regulate cell behavior. Various scaffolds such as HA-based magnetic scaffold, composite scaffold (magnetic polylactic acid nanofibers, hydroxyapatite scaffold of  $\text{Fe}_2\text{O}_3$ ) were prepared and evaluated *in-vitro* and *in-vivo* for tissue regeneration [51]. A calcium phosphate scaffold (CPC) comprising SPIONs (SPIONs@CPC) was fabricated for bone tissue engineering. It was observed that SPIONs increased the human dental pulp stem cells attachment (hDPSC) and spreading, improved bone mineral synthesis, and a 3-fold rise in osteogenic differentiation in contrast to a native CPC. This enhancement was due to the increased microstructure of SPIONs@CPC leading to augmented internalization by the hDPSC cells [76]. Such scaffolds exhibited magnified cell adhesion, proliferation, differentiation, and also enhanced bone healing with antimicrobial effect [9].

Other biomagnetic scaffolds comprising the integrated form of polymers and MNPs have shown the potential application of MNPs in tissue repairing [80,81]. Recently, a magnetic scaffold comprising various polymers (chitosan, HA, and gelatin or bovine serum albumin), calcium phosphate, and MNPs have been prepared for bone tissue engineering. The biopolymers and microporous structures were able to regulate the confinement of simulated biological fluids. Moreover, the fabricated magnetic scaffold exhibited no negative effect on osteoblast cells owing to its biocompatibility [76]. In another study, Torgbo et al. fabricated a microporous nanocomposite scaffold using bacterial cellulose embedded with  $\text{Fe}_3\text{O}_4$  and HA. The fabricated scaffold exhibited superparamagnetic characteristics with superior thermal stability that will be beneficial for bone tissue engineering. The cell culture results revealed that the scaffold was nontoxic and biocompatible together

with positive adhesion and proliferation with the human osteoblast [77].

Furthermore, MNPs can be used to target mechanical sensitive receptors like the Wnt receptor, TREK1 ion channel, integrins, and PDGF receptors [82]. Rotherham et al. investigated the synergistic effect of peptide conjugated MNPs for bone tissue repairing via the Wnt activation in human mesenchymal stem cells [83].

Magnetic cationic liposomes (MCLs) are another MNP based strategy where MNPs were initially integrated with liposomes and later cultured on adipose-derived cells. MCLs have shown potential application in TE due to their tissue repairing ability without using scaffold-based material. These positive charge structures enabled easy interaction with the negatively charged cell lines [51]. MCLs have been used for the building of 3D artificial skeletal muscles via the labeling of myoblast cells under a magnetic field [84].

Magnetolectric scaffold (MS) is another novel approach imparting electrical and mechanical stimulation to the desired cells/tissues under the EMF also used as regenerative medicine. Recently, Mushtaq et al. fabricated 3-D MS comprised of cobalt ferrite@bismuth ferrite magnetolectric NP and poly (l-lactic acid). The fabricated MS was able to generate a localized electric field under EMF (13 mT at 1.1 kHz) leading to improvement (134%) in cell proliferation [85]. In another study, a novel 3-D porous MS encompasses poly (vinylidene fluoride) (PVDF), and  $\text{CoFe}_2\text{O}_4$  magnetolectric NPs was prepared for the efficient proliferation of osteoblast cells. The MS was structurally similar to trabecular bone with a size range of 5 to 20  $\mu\text{m}$ , due to the built-in crystallization process of MNPs with PVDF. It was observed that the fabricated MS promoted the preosteoblasts' proliferation after the application of magnetic field owing to both local magnetolectric and magneto-mechanical response of the MS [86].

#### 5.1.4. Photodynamic therapy

Photodynamic therapy (PDT) is a stimuli-responsive therapy employing photosensitizing agents/drugs. Photosensitizers (PS) are organic or inorganic molecules excited using external light with appropriate wavelength and power results in the delocalization of their ground state electrons to the excited state. These excited electrons produce singlet oxygen radicals called ROS, which damages cancer cells up to 20 nm using near-infrared (NIR) (Fig. 8A) [87]. Despite its safe and effective clinical, PDT faces certain limitations like poor aqueous solubility of PS and lack of selectivity and specificity leading to form aggregates in biological fluid and diminishes the therapeutic efficacy respectively. The therapeutic efficiency of PDT can be synergized by the integration of various nanoformulations with PS owing to their ability to enhance the solubility of PS and augmented cellular uptake [88].

MNPs conjugated/encapsulated with PS have been extensively used for PDT due to their unique properties, wide absorption of NIR light, and low toxicity. Recent studies revealed that MPNs exhibited magnified photothermal transformation efficiency in contrast to other photo absorbers [89].

The literature revealed that MNPs exhibited extraordinary and efficient photodynamic activity in cancer treatment, and

unveiled strong anti-cancer effects on various cancer cell lines like human prostate cancer, breast cancer, and cervical cancer, etc. [3]. Basoglu et al. prepared protoporphyrin IX (PpIX) loaded MLs (221 nm) for the PDT against breast cancer cell line (MCF-7). The cytotoxicity result revealed that the cell viability was reduced to 65% upon incubation with 350 nM of PpIX-MLs at a dark condition where as significant cell death was observed within 5 min of light radiation even at smaller NPs concentration (250 nM) [90]. Further, functionalized MNPs killed cancer cells in a controlled manner due to the deep penetration of NIR results in the photothermal effect i.e., photothermal ablation of MNP. Choi et al. showed the magnified anticancer effect of chlorin e6 (PS) and folic acid conjugated IONPs on the prostate (PC-3) and breast (MCF-7) cancer cells upon irradiation of 660 nm light. The enhanced anticancer effect was due to the deep penetration of light radiation [91]. Moreover, NIR and photothermal ablation of functionalized MNPs can eradicate tumors efficiently via increasing the ROS concentration in tumor cells, reducing the distance between the target site and ROS through mitochondrial targeting. Regarding this, a multifunctional  $\text{Fe}_3\text{O}_4@\text{Dex}/\text{TPP}/\text{PpIX}/\text{ss-mPEG}$  NPs was prepared for the targeted PDT to cancer. The triphenylphosphine (TPP)-grafted dextran conjugated IONPs ( $\text{Fe}_3\text{O}_4@\text{Dex-TPP}$ ) was firstly prepared and then followed by conjugation with PpIX and the GSH-responsive mPEG-ss-COOH. The *in vivo* studies revealed that after i.v administration the internalized NPs were decomposed into  $\text{Fe}^{2+}/\text{Fe}^{3+}$  in lysosomes and then diffused into the cytoplasm. Subsequently, in cytoplasm  $\text{Fe}^{2+}$  reacted with the excessive  $\text{H}_2\text{O}_2$  to produce  $\text{O}_2$  and OH leading to destroy the tumors. Later on, the undecomposed formulation was internalized to the cytoplasm via photoinduction and targeted to mitochondria due to TPP targeting ability. Simultaneously, ROS produced by the Fenton reaction can magnify the therapeutic efficacy of the formulation [92]. Recently, Makole et al. showed the photodynamic antimicrobial chemotherapy of indium porphyrins grafted Ag core-shell MNPs against *Escherichia coli* [93].

These particles have been studied for decades for such applications and few formulations are in clinical trials. Furthermore, in hyperthermal and photothermal cancer therapy MNPs have recently been tested for drug loading and transport to the target tumor [17,94].

#### 5.1.5. Radioimmunotherapy

Radioimmunotherapy (RI) is a combination of antibodies and radionuclides used to treat various cancers. In RI, antibodies are labeled with low doses of radioactive isotopes leading to target specific antigens present on the cancer cells, accumulate the radioisotopes to the targeted cancer cells, and destroy the cancer cells via uninterrupted radiation (Fig. 8B) [6]. Radioisotopes extensively used for the therapeutic application emit  $\alpha$ -,  $\beta$ -particles, or Auger electrons, destruct the DNA by various mechanisms like ROS generation, hamper DNA repairing [95]. However, RI faces certain limitations like poor permeability and radiosensitivity due to the hypoxic nature of the tumor cells enabling less production of ROS [87].

SPIONs are widely used in RI due to the high surface volume ratio, biocompatibility, and easy surface functionalization [95]. However, SPIONs based RI therapy is

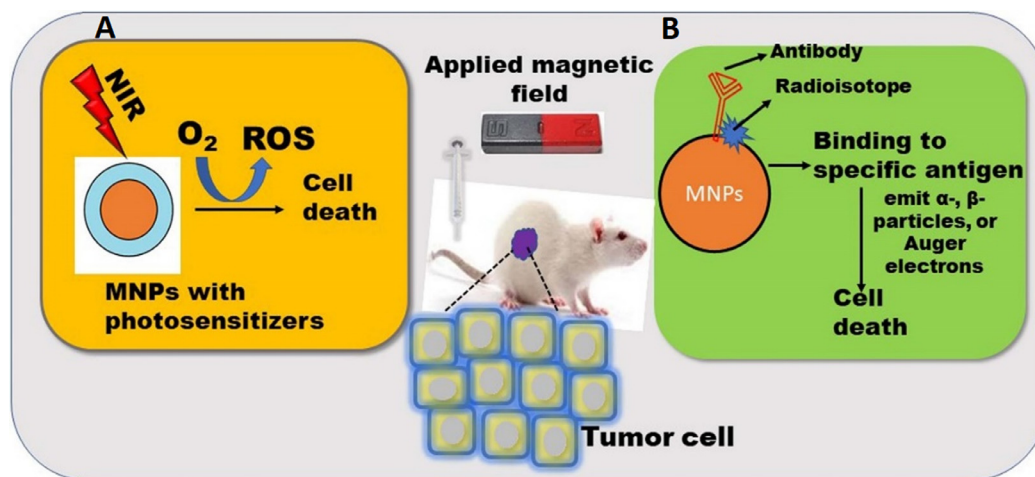


Fig. 8 – Biomedical application of MNPs in (A) Photodynamic therapy; (B) Radioimmunotherapy.

challenging due to the steady decay of the radioisotopes leading to difficulty in avoiding normal cells.  $^{188}\text{Re}$  is the most commonly used radioactive isotope for the fabrication of radioactive SPIONs with a 17h half-life and exhibited in-vivo targeting to the liver [6]. IONPs were also used for the RI via labeling with  $^{165}\text{Ho}$  [96] and  $^{125}\text{I}$  [97] for tumor targeting. In a similar study, SPIONs-trastuzumab conjugate was doped with actinium 225 ( $^{225}\text{Ac}$ ) for RI and MHT of HER2-positive breast cancer cells. It was observed that the  $^{225}\text{Ac}@Fe_3O_4$ -trastuzumab accumulated in the liver, lungs, and spleen, therefore further i.v administration was avoided [98]. This group further extended the work on barium ferrite NPs (BaFeNPs) which also exhibited magnetic properties. These NPs were conjugated with trastuzumab for high affinity towards ligand and cell internalization. In this work, barium was replaced with radium 223 radionuclide ( $^{223}\text{Ra}$ ) in a hydrothermal cation replacement reaction. The obtained radiobioconjugate exhibited cytotoxicity towards the HER2 receptor overexpressing human ovarian adenocarcinoma SKOV-3 cells [99].

#### 5.1.6. Magnetofection

Magnetofection is a synergistic approach, where MNPs are integrated with viral and nonviral vectors for the targeted delivery of genes or gene fragments (DNA) in the presence of EMF [6]. In genetic engineering, more specifically in gene therapy vectors are the carrier for the delivery of nucleic acid in the host genome. Adenovirus, herpes simplex virus, and smallpox virus are some examples of viral vectors. However, these vectors possess some drawbacks like the generation of the immune response, a limited number of genes, random insertion into the host chromosome during gene transfer, and high cost. In the class of non-viral vectors liposomes, NPs, and cationic polymers have been extensively applied. Although such vectors have low transfection efficiency but can have high loading due to their charged surfaces.

MNPs based transfection is advantageous due to the nontoxic nature of the MNPs-gene vector complex and magnified transfection efficiency within a short incubation time. Moreover, this technology delivers genes to the

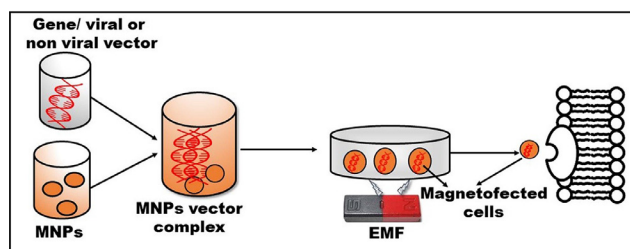


Fig. 9 – MNPs based transfection approach for the magnified gene delivery to the target area by using an EMF.

unpermissive cells by using a low dose of vectors and protects the genes from enzymatic degradation leading to enhance cellular internalization [6]. This technology involves the administration of the MNPs-gene vector complex into the cell line, which is targeted to the specific area by using EMF, resulting to promote endocytosis and transfection (Fig. 9). These magnetically driven structures are also easy to purify from cellular debris during the processing. The magnetofection efficiency can be increased either by dispersion of MNPs in a biocompatible polymeric matrix or by entrapment in metallic or polymeric shells. Moreover, various studies revealed that variation in a magnetic field such as amplitude and frequency [100], speed, and direction [101], also influences the magnetofection efficiency. Regarding this, Zuvin et al. fabricated polyethyleneimine (PEI)-coated cyto-compatible SPIONs for the delivery of nucleic acid to various cancer cell lines such as breast cancer (MCF-7), prostate (DU-145, PC-3), and bladder (RT-4) under varying magnetic field [101]. However, the transfection time (8h) was less while using the PEI approach. Therefore, they developed a novel magnetic actuation system for improved magnetofection by using four rare earth magnets (EMF source) on a rotary table. PEI-coated SPIONs with DNA of green fluorescent protein were used as a model and tested on breast cancer cells (MCF-7). The new system was more biocompatible and possess a short transfection time (1h) [102]. In another study, the magnetofection efficiency of PEI-SPION bearing

plasmid DNA was improved by using a novel magnetic field generator. The tailored formulation is distributed uniformly on the surface of MG-63 osteoblasts via local transfection and without disruption of membrane resulting in augmented magnetofection [103]. Recently, NIH3T3 fibroblast cells have been transfected by MNPs-glycosaminoglycan (GAG)-plasmid (p)DNA trio under a static magnetic field. GAG-binding enhanced transduction (GET) is proposed to proficiently deliver a diverse cargo intracellularly as a non-viral gene delivery system [104].

Commercially OZ Biosciences (France), MEDIBENA Life Sciences (Europe), BOCA Scientific (FL, USA) marketed three different MNPs based formulations for magnetofection encompasses PolyMag (polymer-based MNPs formulation), ViroMag (specific for localized delivery of viral vectors), and DogtorMag (a lipid-based MNPs formulation used to transfect plasmid DNA, antisense oligonucleotide, mRNA or siRNA) respectively. Additionally, OZ Biosciences (France) marketed another commercial formulation NeuroMag which is used to transfect various neurons together with all types of nucleic acid [105].

## 5.2. Diagnostic application of HP-MNPs

### 5.2.1. Cell tracking

Biocompatible MNPs exhibiting enhanced contrasting properties have been explored for cell movement in the in-situ application. This is important for the assessment of retention of cells in the microenvironment and further repeated requirements of treatment in regenerative medicine. Cellular receptors can be labeled with ligand attached MNPs for surface signal generations, which is an *in situ* environment that exhibits resonance and is visualized as contrast molecules. This is explored in the case of stem cell's potential in regenerative medicine, where stem cells labeled with such MNPs are injected into the body and tracked for their habitat/location. SPIONs assembled magnetic nanobubbles were used to label neural stem cells and imaged by ultrasound and MRI [106]. For the treatment of Parkinson's diseases (PD) the role of human adipose-derived stem cells (hASCs) was investigated. The hASCs were labeled with NEO-LIVE™-Magnoxide 797 (magnetic silica core-shell nanoparticle) as per manufacturer protocol. These MNP-hASCs were studied in a 6-hydroxydopamine (6-OHDA)-induced PD mouse model. The maestro imaging of the brain discovered excellent hASCs signals in the *in situ* environments of mice [107]. In multiple sclerosis and amyotrophic lateral sclerosis migration of SPIONs-labeled cells from the site of injection was studied for the safety of injection of mesenchymal stem cells and also in a study of autologous CD34<sup>+</sup> bone marrow cells injected into the spinal cord of patients with chronic spinal cord injury [46]. A detailed description is mentioned in the imaging section showing special insights on MNPs in imaging/tracking.

### 5.2.2. Magnetic bioseparation

Magnetic bioseparation comprises the separation of various molecules from the biological medium/fluids by using magnetic susceptible materials via the application of EMF [108]. It is a simple, cost-effective, and efficient approach in

contrast to conventional methods [17]. MNPs offer various advantages like lower aggregation, enormous surface area, easy modulation under EMF, one-pot separation, and flexible particle size [109–111]. Moreover, the efficiency of magnetic bioseparation can be enhanced by surface functionalization of MNPs with various biocompatible polymers, organic and inorganic biomolecules [109].

MNPs modified with target-specific ligands can selectively capture the target analytes in a solution resulting in preconcentration. This approach is mainly advantageous when analytes are present in lesser concentrations. These MNPs are surface modified with recognition elements selective to the analyte and the binding is governed by various interaction forces like electrostatic, hydrophobic, and van der Waal forces. Further, these preconcentrated/enriched molecules are recovered via the application of EMF, while the non-target analytes are separated. The recovered target analytes are further purified by multiple washing and eluting with washing and eluting buffer solution respectively. Further, MNPs binding sites can be regenerated via incubating in fresh solution (Fig. 10) [111]. This technique is commonly used for the separation of various biomolecules like proteins, nucleic acid, bacteria, and cells. High-affinity nickel-nitrilotriacetic (Ni-NTA) resins like agarose/polyacrylamide etc., have been the first choice for researchers for the separation of histidine (His)-tag proteins for decades. MNPs are equally competing with these resins owing to their magnetic properties. One such example is selective binding and separation of His-tagged human superoxide dismutase 1 (hSOD1) with the loading of 62.0 mg/g on NPs [112]. In another study, Ni-MNPs were also employed to purify this protein by taking advantage of a his-tagged dispersin B (DspB). DspB is a glycoside hydrolase from *Actinobacillus actinomycetemcomitans* which helps in biofilm release [113]. Recently, Minkner et al. investigated the use of Ni-modified MNPs for affinity purification of desired recombinant proteins expressed in the silk worm fat body [114]. Few examples of commercially available magnetic separators are Dynabeads™ magnetic cell separation and MagniSort technology from Thermo fisher and EasySep™ magnetic cell separation by stem cell technologies for the enrichment and isolation of cells from various species.

### 5.2.3. Biosensors

MNPs based biosensing employs the direct integration of MNPs with the transducing elements or dispersion of the MNPs in the sample followed by their attraction by an EMF onto the active detection surface of the (bio)sensor [115]. MNPs based biosensors are advantageous in terms of magnified sensitivity, enhanced signal-to-noise ratio, and reduced analysis time. Different transduction principles like electrochemical, optical, magnetic field and piezoelectric are used for biosensing purposes. Based on divergent transduction principles various MNPs based sensors have been developed. Several types of MNPs whether bare or modified have found applications in various types of sensors. Gold-coated Fe<sub>3</sub>O<sub>4</sub>, Fe<sub>3</sub>O<sub>4</sub>@silica, Fe<sub>3</sub>O<sub>4</sub> functionalized reduced GO-NPs, Fe<sub>3</sub>O<sub>4</sub>@gold-multiwalled carbon nanotube-chitosan, Fe<sub>3</sub>O<sub>4</sub>@silica/multiwalled carbon nanotube have been mainly used in electrochemical detections.



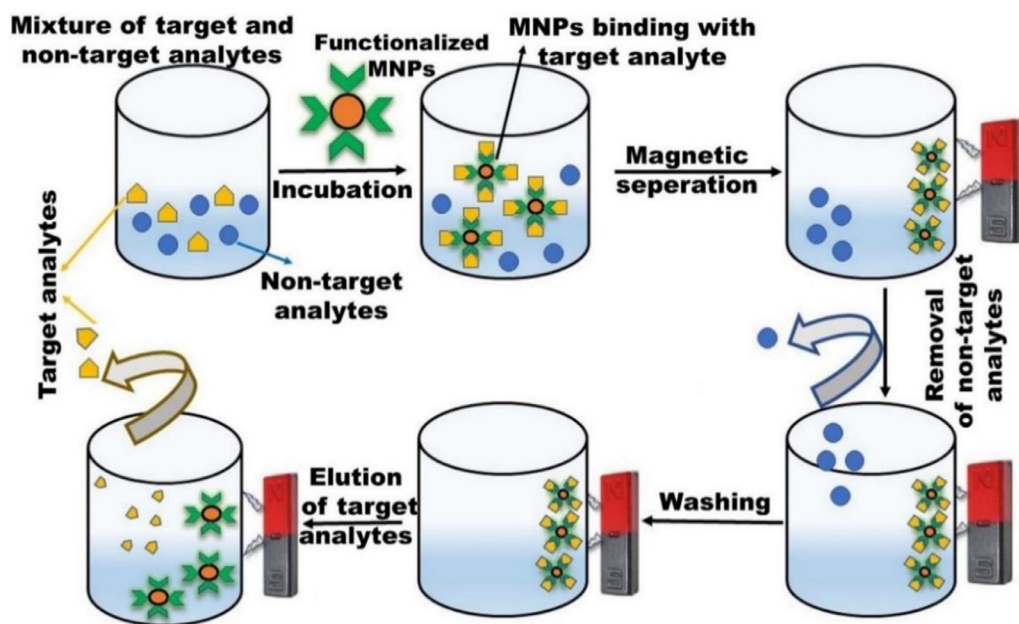


Fig. 10 – Bioseparation of the target analyte by using MNP.

The electrochemical (EC) method measures voltage, current, and impedance, generated via the immunochemical interaction between analytes and electrodes. Here, MNPs immobilized with various molecules like enzymes, antibodies, or proteins are attached to sensor electrodes for the detection of various biomarkers with minimal interference together with amplified responses [116]. This method is widely used clinically and therapeutically due to its cost-effectiveness, easy operation, enhanced accuracy, and sensitivity [17]. Based on the operating principle EC method can be further classified into amperometric, capacitive, chemiresistive, potentiometric, and voltammetric. Fig. 11 summarizes various functionalized MNPs like gold-coated  $\text{Fe}_3\text{O}_4$ , gold-coated  $\text{Fe}_3\text{O}_4@SiO_2$ ,  $\text{Fe}_3\text{O}_4@SiO_2$ , Carbon nanotube functionalized MNPs,  $\text{Fe}_3\text{O}_4$  integrated with GO, nano biocomposites of chitosan-  $\text{Fe}_3\text{O}_4$  have been used for EC based sensing [115,117,118]. CEA, clenbuterol, organochloride pesticides, Metronidazole, Streptomycin, Uric acid, Glucose,  $\alpha$ -fetoprotein, Ochratoxin A are among some analytes detected by the EC method.

The optical method is a diverse technique for biosensing due to the abundance of various detection principles like absorption, dispersion, fluorescence, phosphorescence, chemiluminescence, and refraction, etc. Based on the principle various optical devices like fluorescence spectroscopy, surface-enhanced Raman spectroscopy (SERS), electrochemiluminescence, colorimeter, surface plasmon resonance (SPR), interferometry is used (Fig. 11) [17,115]. Gold, silver, and silica-coated MNPs exhibit plasmon properties which are used mainly in optical-based methods. A-ferritin, Thrombin, IgG, Ochratoxin A, E.coli. have been detected by optical methods. Magnetic behavior of such NPs has also been explored for the sensing of Endoglin in human urine, Interleukin 6 and Cancer Cells, protease, DNA by Giant magneto-resistive [119], Magneto-Optical fiber, and Hall

sensors [120]. Although giant magnetoresistance is a complex phenomenon yet in simpler words change in magnetic resistance is observed before and after the application of a sample. e.g., in the case of protease assay some peptides conjugated with MNPs were immobilized on a sensor strip, and data was recorded. These were further treated with protease enzyme which cleaved the peptide and liberated the MNPs from the sensor surface, resulting in resistance to the magnetic field. The magneto-optical method records the change in refractive index of the system before and after binding of MNPs on the optical fiber surface. The hall sensors can be made on a silicon wafer with the growth of materials like InSb which exhibits hall coefficient. Likewise, for all other chip-based biosensors the surface passivation is required to bind the recognition molecule. Further, the sensor chip is modified with a recognition element specific to the target analyte, and the signal is recorded.

Quartz crystal microbalance has been used immensely for the sensing of a minute change in the mass of biomolecules. The recognition element is immobilized on the quartz surface which brings the change in the resonance frequency of these crystals. Change in frequency is correlated with the mass change on the surface of the biosensor chip. Various analytes have been detected using this method e.g., avian influenza virus H5N1, C Reactive Proteins, Myoglobin, and E. Coli.

#### 5.2.4. Imaging

Various imaging techniques have been established to get acquainted with human and animal physiology and anatomy for a couple of decades. These techniques are nuclear magnetic resonance (NMR), magnetic resonance imaging (MRI), optical imaging, positron emission tomography (PET), single-photon emission computer tomography (SPECT), computer tomography (CT), magnetic particle imaging (MPI), ultrasound imaging (UI), photoacoustic imaging

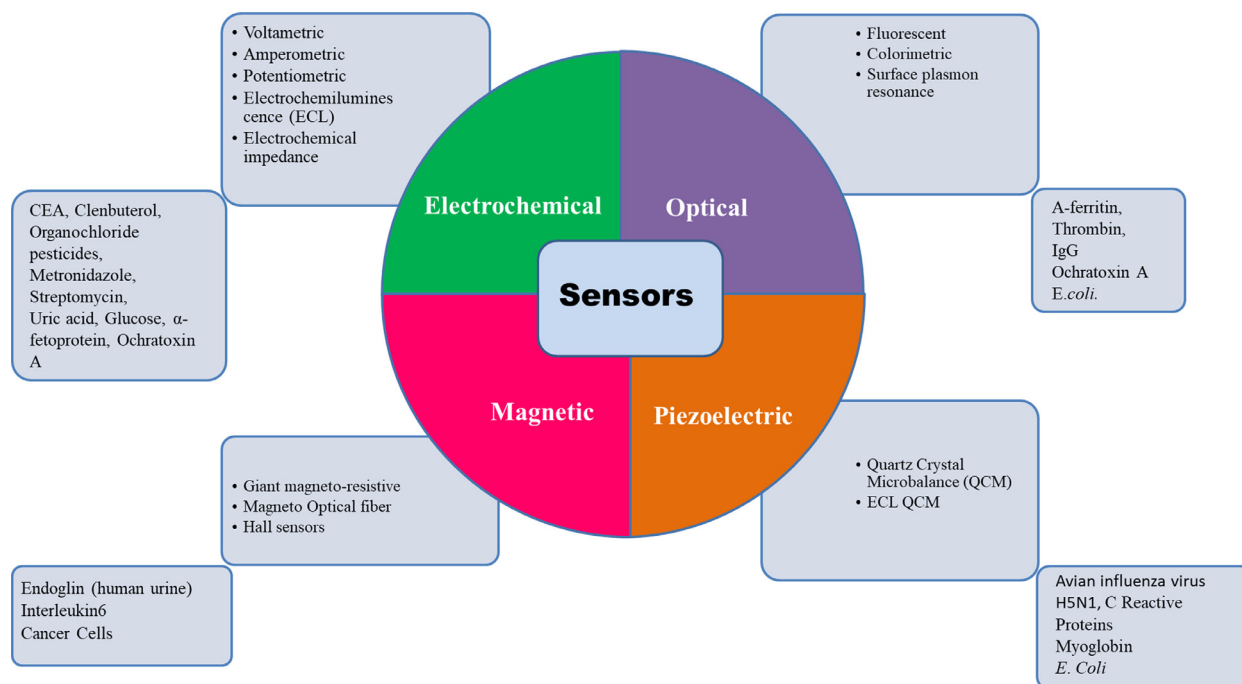


**Fig. 11 – Various biomarkers have been investigated utilizing MNPs. Most explored biosensors are based on electrochemical methods having a wide range of applicability. This figure summarizes the possible methods of biosensor development.**

(PAI) [1,116,121]. However, MRI and CT give the anatomical particulars while, optical imaging, PET, SPECT, MPI, and PAI provide molecular details. Moreover, the individual technique is no able to the extensive imaging due to their respective limitations (Table 6). Therefore, multimodal imaging techniques (MMI) have been designed for further magnified resolution and sensitivity in conjunction with complementary knowledge [116,122]. MNPs specifically SPIONs are extensively used for MMI via the fusion of MRI with other imaging techniques due to high surface volume ratio, versatility, and easy surface functionalization [1]. In this section, various single imaging techniques and MMI techniques will be discussed.

**Imaging techniques: Nuclear magnetic resonance imaging:** Magento pharmaceuticals are a new class of pharmaceuticals used for the clinical diagnosis by the administration of these into the patients to observe the image contrast difference between the normal and disease tissue. Endorem® and Resovit® (marketed formulations) have been used as an NMR imaging contrast agent for the diagnosis of various diseases like cardiac and brain infracts, and liver injury or tumors. Various molecules like protein, peptides, and oligonucleotides have been cross-linked with the aminated MNPs for the recognition of inflamated pathological structures [2].

**Magnetic resonance imaging:** MRI is one of the most sensitive and non-invasive techniques for three-dimensional deep tissue/organ imaging. This technique is extensively used for the clear anatomical presentation of non-bony or soft tissues due to accuracy, outstanding signal-to-noise ratio, magnified spatial resolution [44,121]. In this technique, the protons present in water molecules inside the body become excited and aligned parallelly in the direction of the applied

magnetic field with a particular radio frequency (RF) pulse. On removing the magnetic field, protons get relaxed by releasing their energy while generating an RF signal and realign themselves at their thermal equilibrium state.  $T_1$  and  $T_2$  are longitudinal and transverse components of magnetization vectors respectively. Either  $T_1$  or  $T_2$  relaxation times are measured by receiver coils to produce an MR image by a computer algorithm [116,123]. The imaging quality and diagnostic sensitivity of MRI are improved by using contrast agents. Paramagnetic gadolinium (Gd) combined with other chelating agents is widely used as  $T_1$  contrast agents, modify the  $T_1$  relaxation time resulting in brighter tissues/organs. However, Gd use is limited due to inherent toxicity, short half-life, inferior cellular uptake [1,116].

MNPs are potentially used as a contrast agent and magnify the imaging resolution by shortening the  $T_1$  and  $T_2$  relaxation time of adjoining protons. However, MNPs are commonly used as negative contrast agents due to the larger relaxation of  $T_2$ . SPIONs and ultra-small SPIONs (USPIONs) have been extensively used for MRI due to their biocompatibility, stability, biodegradability, and magnified uptake by RES enabling the identification of smaller lesions easily. The efficiency of MNPs as a contrast agent is dependent on the size, surface properties, shape, and composition of MNPs [121]. Studies revealed that the large-sized SPIONs (16–200 nm) exhibited increased magnetization and  $T_2$  relaxation, while small-sized MNPs (<10 nm) showed enhanced  $T_1$  relaxation. Moreover,  $T_2$  relaxivity can be enhanced by adjusting the magnetization and diameter of MNPs, which is dependent on MNPs' shape [116]. Ellipsoidal MNPs possess homogeneous magnetization, while distorted shape gives dissimilar magnetization [121].

**Table 6 – Comparative analysis of various imaging technique [1,121,148,195].**

Technique	Source	Spatial resolution	Advantage	Limitation
Nuclear magnetic resonance	Radiowaves		The unique and highly sensitive technique for the detection of small molecule	A large amount of purified substance is required
Magnetic resonance imaging	Magnetic field and radiofrequency waves	20–100 $\mu\text{m}$	Magnified resolution together with an outstanding signal to noise ratio enabling clear anatomical presentation of non-bony or soft tissues	The costly instrument, poor sensitivity at the cellular/molecular level, and faces endogenous artifacts
Optical	Near-infrared light	>0.3 $\mu\text{m}$	Concomitant detection of various biomarkers and molecular due to extensive availability of fluorophores, inexpensive instrument, and safe	Insufficient anatomical information due to restricted light penetration into the deep tissues, and clinically not available
Positron emission tomography	Ionizing radiation ( $\gamma$ and $\beta$ )	1–2 mm	Easily detect cancer, non-cancerous cells, and neurological disorder at an early stage and lesser probability of infection during the medical process	Employs ionizing radiation leading to adverse effects on the normal cells, expensive machine, poor resolution, and inefficient for anatomical details
Single Photon Emission Computer Tomography	Ionizing $\gamma$ radiation	1–2 mm	Simultaneous visualization of multiple biological processes at the molecular level, lesser expensive than PET and higher sensitivity with deep penetration	Poor spatial resolution, and inefficient for anatomical details
Computer tomography	X-ray	50–200 $\mu\text{m}$	Magnified resolution along with three-dimensional anatomical images of various organs	Narrow functional details, poor diagnosis of soft tissues, and expensive machine
Magnetic particle imaging	MNPs (iron-oxide)	<1mm	Highly sensitive, fast, safe, and real-time imaging without background signals	Insufficient anatomical information, and overheating under high magnetic field
Ultrasound imaging	Ultrasound waves	50–500 $\mu\text{m}$	Low cost, safe, real-time imaging without any harmful radiation, and coverage of the large area in a single scan	Poor resolution and sensitivity, limited penetration, and narrow functional details
Photoacoustic imaging	Photoacoustic waves	<1mm	The safe, magnified resolution, coverage of a large area, and provides functional imaging of various organs	Required exogenous contrast agents in absence of biological chromophores, poor penetration depth, and inefficient for anatomical information

Various MNPs such as metal oxide NPs, carboxylated PEG-coated magnetic ferrite, monoclonal antibody labeled pegylated  $\text{Fe}_3\text{O}_4$  for colon cancer in a mouse model, lactobionic acid (LA) modified chitosan-coated SPIONs (CS-LA@SPIONs) for hepatic cancer, chloride channel buthotoxin (CTX) modified pegylated  $\text{Fe}_3\text{O}_4$  for glioma cells has been studied [116,124,125]. Furthermore,  $T_1$  and  $T_2$  relaxivity have been magnified by preparing the various metal or metal alloy nanohybrids, and via doping various metals such as manganese (Mn), zinc (Zn), copper (Cu), and europium (Eu) in the lattice of  $\text{Fe}_2\text{O}_4$  and  $\text{Fe}_3\text{O}_4$  NPs [124,126]. The results revealed that the nanocomposite exhibited magnified  $T_1$  contrast in contrast to Gd and SPIONs [127]. Ferumoxides, ferristene and ferumoxtran-10, fetumoxyto, ferumoxsil, abdoscan, and ferucarbotran are commercially available MNPs used as contrast agents [105]. However, the MRI technique is incapable to diagnose molecular events like gene expression and protease activity [128].

**Optical imaging:** The optical imaging technique is extensively used for the diagnosis of early-stage cancers,

fluorescence-guided surgery, immunostaining, and endoscopic imaging [1,8]. This simple technique measures change in the incident light as a result of absorbance, reflectance, bioluminescence, and fluorescence by sample concentration. Near-infrared fluorescence (NIRF, 700–1000 nm) is the most commonly used source due to its ability to pass through the tissues resulting in complete body tomography [1]. Various optical imaging agents like gold NPs, lanthanides, organic fluorochromes, quantum dots are commonly used for *in vivo* detection [122]. Biological tissue has some inherent fluorescence when excited in the UV–vis region and hence produces a poor-quality image in terms of contrast. Therefore, NIRF detection provides excellent contrast as excitation in this region avoids the background fluorescence of such tissues. The versatility, non-toxicity, sensitivity, and cost-effectiveness make this technique effective for *in vivo* applications [1]. However, optical signals are very weak and have poor depth of penetration/imaging, easily clear from the body [122].

**Positron emission tomography:** PET is a biomolecular imaging technique used to diagnose the biological metabolic process.

This technique recognizes the gamma rays which are emitted from the radionuclide administered inside the body [116]. Positrons emitted by radio-isotopes (interact with tissue and generate two photons which are detected by a scintillation camera placed near the samples in various arrangements. This technique employs the formation of MNPs complex with the required isotope by using a polycarboxylate macrocycle chelating agent such as 1,4,7-triazacyclododecane-N, N', N''-triacetic acid (NOTA) and 1,4,7,10-tetraazacyclododecane-N, N', N'', N'''-tetraacetic acid (DOTA) [1]. The tailored MNPs are deposited to the living tissues and provide the bright image which is captured by the PET scanner [129]. This technique can easily diagnose disease conditions at an early stage [121] but exhibits poor spatial resolution [129]. The PET imaging technique is mainly dependent upon the radionuclide half-life and positron energy. Radionuclide with optimal half-life and smallest maximum positron energy is used for imaging eg.  $^{64}\text{Cu}$ ,  $^{18}\text{F}$ ,  $^{111}\text{In}$ ,  $^{124}\text{I}$ ,  $^{89}\text{Zr}$  [1].

**Single photon emission computer tomography:** Similar to PET, SPECT is also a nuclear imaging technique that provides important biological information with magnified sensitivity [121]. This technique utilizes radioactive tracers as contrast agents to acquire images in 2D or 3D format via a computer program. The basic difference between PET and SPECT is the use of specific radionuclides like  $^{67}\text{Ga}$ ,  $^{125}\text{I}$ ,  $^{111}\text{In}$ ,  $^{131}\text{I}$ ,  $^{99\text{m}}\text{Tc}$ , and  $^{201}\text{Tl}$  for SPECT imaging. Among all radionuclides,  $^{99\text{m}}\text{Tc}$  has been extensively used for imaging owing to less expensive and more available than PET [1]. Similar to PET, this technique also exhibits a poor spatial resolution [129].

**Computer tomography:** CT is an advanced version of X-ray imaging, where multiple X-ray images are combined by computer software to make a tomography of anatomic images of various tissues like blood vessels, bones, and stomach [121]. This technique employs passing the X-rays through the tissues and measured the different X-ray attenuation coefficients of various organs resulting in high spatial resolution images of the body by 3D slicing technology [1,3,128]. This technique is clinically used widely due to low cost, readily available, small acquisition time, extensive tissue penetration, and magnified spatial resolution [128]. Additionally, various images from different angles can be captured and overlying structures can be easily eliminated from the developed images enabling recognition of abnormalities [116]. Various contrast agents like bismuth, gold, iodine, platinum, tantalum, and ytterbium are commonly used [8]. These contrast agents block X-rays in a specific part to construct CT images [128]. However, these contrast agents are rapidly excreted from the body resulting in a short half-life. Iodine based contrast agent faces some side effects such as etching, vomiting, and anaphylactic shock [128]. Recently, gold NPs are extensively used as a CT contrast agent due to their biocompatibility, and tumor targeting. Due to the high molecular weight, Gold NPs exhibited a magnified X-ray absorption coefficient in contrast to conventionally used iodine-based CT contrast agent, omnipaque [1,128].

**Magnetic particle imaging:** MPI is an MNP-based imaging technique where SPIONs are not just assistive contrast agents, but the sole source for sending the signals out to the imaging system. This technique provides a quantitative estimation of MNPs inside the body without background signal [130] and

utilizes two different magnetic field regions [131]. The first region comprises a high magnetic field resulting in the saturation of MNPs magnetic moment and aligns MNPs parallel to the EMF. The second region is the zero magnetic field are also known as a field-free point (FFP), where the MNPs magnetic moment is randomly aligned. MNPs located in the FFP region can easily generate MPI images [132]. MPI is widely used in various biomedical applications like measurement of blood flow, imaging of various organs and tumors, and MPI-guided hyperthermia [131,133]. This real-time imaging technique is advantageous owing to its speed, safety, magnified penetration depth, and high resolution. However, the clinical use of MPI is hampered due to lack of anatomical details and overheating in presence of higher EMF [17].

**Ultrasound imaging:** This imaging technique is extensively used for the detection of various diseases, and angiography due to real-time imaging, low cost, and safety [134]. This technique relies on the absorption and reflection of ultrasound (US) waves by various contrast agents like microbubbles, liposomes, and perfluorocarbon droplets [130,135]. However, the clinical application of UI is hampered due to its poor sensitivity, resolution, and penetration [8].

**Photoacoustic imaging:** Photoacoustic imaging (PAI), also known as thermoacoustic or optoacoustic imaging is a hybrid technique that utilizes UI and optical imaging. The principle of PAI relies on measuring the acoustic waves which are originated from the thermoelastic expansion of tissues after the absorption of light energy (680–970 nm), and further acoustic waves are processed to form tissue images [131]. Hemoglobin and melanin are the most commonly used PAI contrast agents owing to their substantial optical absorptivity, and biocompatibility [1]. However, in some diseases, these chromophores are not available then exogenous contrast agents like gold NPs [136], gold nanocages, gold nanorods [134], IONPs [131], indocyanine green [137], QDs [138], and single-wall carbon nanotubes [139] are used. PAI is fast, safe, cover a larger area in a single scan, and is used to visualize functional imaging of various tumors and organs [116,131]. However, the clinical application of this technique is limited due to poor penetration [131] and inefficient anatomical imaging [1].

**MNP-based multimodal imaging:** An individual imaging technique is incapable to provide extensive anatomical or molecular information due to their respective limitations (Table 6). Therefore, multimodal imaging techniques (MMI) have been designed via the combination of different imaging techniques for further magnified resolution and sensitivity. In this section principles, composition, and advantages of various MNP based MMI, techniques are explained (Table 7).

**T<sub>1</sub>-T<sub>2</sub> MRI dual imaging:** Traditionally independent use of MRI contrast agents gives inaccurate results and provides either bright (T<sub>1</sub>) or dark (T<sub>2</sub>) signals. Moreover, the accuracy and sensitivity of MRI images are also affected by endogenous artifacts like air, blood clots, fat, calcification, and hemorrhages, air [130]. T<sub>1</sub>-T<sub>2</sub> dual MRI imaging is the best alternative to overcome such vagueness by using dual-mode NP contrast agents (DMCA). This dual imaging provides both T<sub>1</sub>-weighted and T<sub>2</sub>-weighted MRI images with improved

**Table 7 – Magnetic nanoparticles for multimodal imaging.**

Multimodal imaging	Composition	Advantage	Limitation	Ref
T <sub>1</sub> -T <sub>2</sub> MRI	Direct conjugation /labeling of T <sub>1</sub> agents with the T <sub>2</sub> agents (MNPs or metallic ferrites), inserting the T <sub>1</sub> agents inside the MNPs, and magnetically decoupled T <sub>1</sub> and T <sub>2</sub> contrast agents	No image mismatch between separate instrument without a discrepancy between T <sub>1</sub> and T <sub>2</sub> penetration depth, T <sub>1</sub> weighted imaging gives magnified resolution in tissues and T <sub>2</sub> weighted imaging provide accurate details about the lesions without endogenous artifact	Complicated process	[130,135,142]
Optical-MRI	Physical or chemical conjugation of fluorescent dyes with the MNPs	Provide anatomical and functional detail of all molecular events	Long chemical linkers are required to prevent quenching	[1,128,130]
PET/SPECT-MRI	SPION (MRI agent) conjugated with the radionucleotide through chemical conjugation	Impart anatomic information with a high spatial resolution and accurate molecular imaging of a specific tissue due to high sensitivity	The sensitivity of two imaging techniques must be fully considered while designing such probes	[121,128]
CT-MRI	Gold shells on iron oxide MNPs (GION) to build a dual imaging probe for CT-MRI with relatively higher T <sub>2</sub> relaxivity	Provides anatomical imaging of hard and soft tissues with the magnified resolution, deep information about the brain and pituitary tumors	Poor functional imaging	[8,121,128]
UI-MRI	Conjugation of SPION (MRI contrast) with the microbubbles (UI contrast)	Magnified resolution		[134]
PAI-MRI	A fusion of PAI contrast agent with MNPs (MRI contrast)	Provides anatomical and functional imaging simultaneously		[156]

quality and accurate interpretation of MRI signals. These DMCAAs can be designed by different techniques via using the unique properties of MNPs. The first technique comprises the direct conjugation /labeling of T<sub>1</sub> agents (Gd or Mn) with the T<sub>2</sub> agents (MNPs or metallic ferrites [121]. Magnevist® (Gadopentetate dimeglumine), a commercial Gd-based T<sub>1</sub> contrast agent which is covalently linked with dopamine coated SPIONs [130]. In a study, the T<sub>1</sub> contrast agent was directly conjugated on the surface of MNPs. The resultant formulation exhibited both T<sub>1</sub> and T<sub>2</sub> effects resulting in-vivo T<sub>1</sub>-T<sub>2</sub> MRI dual imaging with magnified clarity and contrast of MRI images [140]. Another method includes the insertion of the T<sub>1</sub> agents inside the MNPs enabling to enlargement of the magnetic strength of both contrast agents [121]. Gd<sub>2</sub>O<sub>3</sub> (T<sub>1</sub> contrast agent) was embedded inside the IONPs resulting in MRI dual imaging. The *in vivo* results revealed that the tumor to liver contrast ratio was significantly increased ~83% and 137% for T<sub>1</sub> and T<sub>2</sub> respectively [141]. Magnetically decoupled T<sub>1</sub> and T<sub>2</sub> contrast agents are another technique to achieve simultaneously T<sub>1</sub> and T<sub>2</sub> weighted images [142]. This technique employs the insertion of a non-magnetic spacer like silica between the T<sub>1</sub> (shell; Gd or Mn) and T<sub>2</sub> (core; MNPs) to diminish the magnetic interaction between T<sub>1</sub> and T<sub>2</sub> [130]. Recently, this type of dual imaging was achieved by developing Fe<sub>3</sub>O<sub>4</sub>@mSiO<sub>2</sub>/PDDA/BSA-Gd<sub>2</sub>O<sub>3</sub>-AS1411 MRI probe [143]. Here, Fe<sub>3</sub>O<sub>4</sub> NPs were used as core (T<sub>1</sub>), bovine serum albumin modified Gd<sub>2</sub>O<sub>3</sub> NPs were used as a shell (T<sub>2</sub>), silica was used as a spacer to coat the Fe<sub>3</sub>O<sub>4</sub> NPs and AS1411 aptamer coating was used for further in-vitro targeting to

tumor cells. The resultant formulation exhibited enhanced *in-vivo* MRI imaging.

Recently, MNP based T<sub>1</sub>-T<sub>2</sub> MRI dual imaging was achieved by fabricating bull serum albumin modified Fe<sub>3</sub>O<sub>4</sub> NPs (BSA@Fe<sub>3</sub>O<sub>4</sub>). The synthesized NPs exhibit different MRI contrast which depends on the dispersion medium. The synthesized USPIONs showed a T<sub>1</sub> contrast effect with high relaxivity ( $r_{1}=6.99 \text{ mM}^{-1} \text{ s}^{-1}$ ) but exhibited increased  $r_{2}$  relaxivity upon aggregation. This tailored formulation exhibited magnified diagnostic sensitivity and precision [144].

*MRI-optical dual imaging:* This dual imaging technique has overcome the limitation of both techniques (Table 6). MRI is the best technique for anatomical imaging but poor to diagnose molecular events whereas optical imaging provides functional detail of all molecular events. Hence, by combining these two approaches overall imaging quality can also be improved [128]. This dual imaging technique comprises the conjugation (chemical or physical) of fluorescent dyes with the MNPs [130]. Organic dyes (such as cyanine (Cy5.5), rhodamine B, and isothiocyanate (FITC) or synthetic/inorganic semiconductor quantum dots (QDs) have been conjugated to MNPs for such applications. However, direct conjugation via using a short distance cross linker or adsorption on functional groups on these MNPs may quench the fluorescent signals. This can be overcome by employing thicker coating agents, or longer chemical linkers resulting in increased distance between MNPs and fluorescent molecules enabling minimum quenching [1]. In a study, ultrasmall Fe<sub>3</sub>O<sub>4</sub> MNPs (2–3 nm), and NIR emissive semiconducting polymers (PFBT and

PFTBT), were integrated into amphiphilic polymers bearing carboxylic acid groups in one-step synthesis. The results revealed that the tailored formulation exhibited MRI-optical dual imaging [145]. Recently, phospholipid-PEG coated MNPs were synthesized, and further dialkylcarbocyanine dye was physically adsorbed on the MNPs surface. The *in-vitro* and *in-vivo* results revealed that the tailored formulation exhibited magnified MRI and fluorescence signals [146].

**PET-MRI dual imaging:** MRI is a unique imaging technique that presents the anatomy of non-bony or soft tissues with high resolution but incapable to furnish the molecular and functional details [121]. PET is a sensitive nuclear imaging technique used to detect various disorders at an early stage but suffers from poor spatial resolution [116]. PET-MRI hybrid technique synergistically recompenses the stated limitation. This MMI comprises SPIONs (MRI agents) conjugated with the radionuclide through chemical conjugation [128]. This dual imaging is advantageous and synergistic, as MRI offers anatomic information with high spatial resolution, and PET offers accurate molecular imaging recording radionuclide emitting positrons to illuminate the functional biological process. However, the sensitivity of two imaging techniques must be fully considered while designing such probes. The integrated probe should offer a sufficient dose of radiotracers for PET imaging, and high MRI contrast for MRI [1]. SPIONs and 18F-Fluorodeoxyglucose have been conjugated for imaging myocardial infarction in rats by MRI and PET. As mentioned previously in the MRI section, IONPs have been approved by FDA and can be further reduced by size & doped with manganese, zinc, and cobalt to increase their contrast-enhancement by gaining superior magnetic anisotropy. In a study,  $^{124}\text{I}$  radionuclides were conjugated with serum albumin coated Mn-doped ferrite NPs and applied as PET/MRI dual imaging agents for delineated small sentinel lymph nodes mapping [147]. In another study, polyaspartic acid-coated  $\text{Fe}_3\text{O}_4$  NPs were conjugated with  $^{64}\text{Cu}$  radionuclides and DOTA stabilizing material for *in vivo* targeting of tumor xenografts to provide both MRI and PET images [148]. Recently, oleic acid-coated IONPs were labeled with  $^{68}\text{Ga}$  for dual PET/MRI imaging of the prostate. Further, the glutamate-urea-lysine peptide was used for targeting prostate-specific membrane antigen (PSMA). The dual image results revealed high uptake of the NP by the PSMA-positive tumor cells with magnified resolution [1].

**SPECT-MRI dual imaging:** Similar to PET, SPECT imaging is also not capable to provide anatomical information and exhibits poor spatial resolution [129]. Hence, complementary techniques such as MRI or CT come into the role to magnify the resolution. The radionuclides used in PET /SPECT can be combined with the contrast agents used in MRI/CT. This synergistic approach compensates each technique limitation with better contrast and imaging. Additionally, this integrated approach circumvents multiple anesthesias dosage enabling fewer errors and reduces the associated pain [128]. The SPIONs can be modified with radiotracer and further by targeting ligands for specific localization and signals in cancers even at pico-molar concentration. Various MNP based SPECT-MRI dual imaging have been explored for the diagnosis of various diseases. In one study, cyclic RGP peptide anchored USPIOs were radiolabeled for early cancer diagnosis [135]. In another

study, bisphosphonate chelate stabilized  $^{99\text{m}}\text{Tc}$  loaded IONPs have been prepared for cardiovascular imaging via MRI/SPECT dual-mode imaging [149]. Recently,  $^{99\text{m}}\text{Tc}$  labeled USPIOs with zwitterion coating were fabricated for tumor diagnosis. The results revealed that the tailored formulation exhibited excellent imaging due to the SPET-MRI dual-mode [150]. However, technically operating MRI-SPECT for simultaneously dual imaging is a challenge than the PET/MRI development. The artifacts induced by a gamma camera in the MR images and accommodating a SPECT scanner within an MR instrument is a design challenge yet. However, PET detectors have been incorporated within MRI scanners [1].

**CT-MRI dual imaging:** CT and MRI are excellent anatomical imaging techniques and provides high-quality scans from hard and soft tissues respectively [121]. However, Both techniques provide anatomical detail but poor in functional imaging. Therefore, the combined strategy of CT and MRI overcome the limitation of individual techniques and provides simultaneous anatomical information for efficient diagnosis with magnified resolution. Furthermore, this hybrid technique reduced the dose of the administered contrast agents resulting in lesser adverse effects [1]. This hybrid dual imaging comprises gold shells on iron oxide MNPs (GION) to build a dual imaging probe for CT-MRI with relatively higher  $T_2$  relaxivity [128]. In a study, PEI stabilized  $\text{Fe}_3\text{O}_4$ /gold MNPs have been synthesized and explored for targeted dual-mode MRI-CT imaging of the tumor. The results exhibited enhanced relaxivity with a superior X-ray attenuation coefficient leading to amplify both imaging contrast [151]. In another study, tailored GIONs were tested in animals bearing liver disease for MRI and CT imaging. The results revealed a magnified contrast for both MRI and CT images [152].

**UI-MRI dual imaging:** This dual imaging technique is based on the integration of SPIONs with the UI contrast agent leading to enhance the magnetic resonance and US signals. SPIONs loaded microbubbles are widely used for this dual imaging enabling to improve the diagnostic application via increasing the backscatter signals of US waves [134]. Park et al. developed UI-MRI dual imaging probe via the interaction of SPIONs with the microbubbles [153]. Yang et al. prepared a yolk-shell microsphere by using  $\text{Fe}_3\text{O}_4$  as a core for UI-MRI dual imaging. The imaging results revealed that the tailored formulation exhibited superior dual imaging [154]. Recently, Chen et al. fabricated silica-coated poly (lactic-co-glycolic acid) (PLGA) hybrid nanovesicle loaded with an antitumor drug,  $\text{Fe}_3\text{O}_4$ , and perfluorocarbon for the UI-MRI dual imaging. The tailored formulation exhibited magnified anticancer efficacy with superior dual imaging [155].

**PAI-MRI dual imaging:** This dual imaging technique encompasses the fusion of extrinsic PAI contrast agents with the MNPs (MRI contrast agent) enabling them to provide complementary functional and anatomical imaging with diagnostic accuracy [156]. Ji et al. prepared gold-coated IONPs for the PAI-MRI dual imaging. The synthesized core-shell nanostructure showed excellent dual imaging [1]. Recently, IONPs loaded liposomes were prepared to increase the sensitivity of the PAI-MRI dual probe. The tailored probe exhibited  $2.6 \times$  and  $3.8 \times$  higher signals for PAI and MRI respectively [157]. Yang et al. prepared  $\text{Fe}_3\text{O}_4\text{-Cu}_2\text{O}$  NPs as a magneto-photoacoustic dual probe for the quantitative

estimation of hydrogen sulfide in colorectal cancer. The results revealed that the dual probe was an effective contrast agent for the diagnosis of colon cancer [158].

## 6. Pharmacokinetic, and biodistribution of HP-MNPs

MNPs are designed for *in vivo* delivery of therapeutic modalities to the desired site for the treatment of various diseases. Moreover, these are designed to augment the systemic bioavailability of drugs with biocompatibility and enhanced efficacy. However, there may be some pharmacokinetic alterations in the parent therapeutic modalities which may lead to toxic/side effects [36]. Therefore, the *in vivo* fate of MNPs needs to be addressed to figure out the biological behavior, interaction with the living organism, and efficacy.

MNPs are usually biodistributed in liver (~80%–90%), spleen (~5%–8%), and bone marrow (~1%–2%) [159]. The pharmacokinetics and biodistribution of MNPs are significantly influenced by various factors like physicochemical properties and surface functionalization of MNPs [36]. Additionally, routes of administration, biological fluid composition, and opsonization also affect the various pharmacokinetic parameters like plasma half-life ( $T_{1/2}$ ), distribution, and elimination [129,160].

### 6.1. Factors affecting the pharmacokinetics and biodistribution of HP-MNPs

#### 6.1.1. Size and polydispersity

Particle size plays an important role in the determination of various pharmacokinetic parameters. MNPs smaller than 10 nm are prone to extravasation and renal clearance whereas, larger particles can be easily opsonized and eliminated by the liver (>100 nm), and spleen (200–250 nm) leading to decreased  $t_{1/2}$  [36,160]. Therefore, the particle size between 10 and 100 nm is optimal for prolonged systemic circulation and access to other organs like tumors, brain, lymph nodes, heart, etc. [161]. However, some portion of NPs exists in aggregated form even after within the size range, which influences the MNPs pharmacokinetics. This aggregation is measured in the form of the polydispersity index (PDI) usually in the range of 0.05–0.7.  $PDI < 0.05$  portrays that the NPs are monodispersed, whereas  $PDI > 0.7$  presents the polydispersity of NPs. also influences the systemic circulation of NPs. To achieve prolonged circulation and proper biodistribution the PDI value should be the preferable minimum [18].

#### 6.1.2. Surface charge and shape

It has been observed that surface charge influences the *in-vivo* therapeutic efficacy of MNPs via adsorption of plasma protein onto the MNPs surface and binding of MNPs to the non-specific sites [162]. The nature of the surface charge depends on the chemical composition and surface functionalization of NPs. MNPs with amine groups possess a positive charge, while the carboxyl, hydroxyl, and sulfate groups provide a negative charge to the MNPs [18]. Moreover, charged particles are more prone to hepatic and renal clearance in comparison to

neutral particles [163]. Positively charged particles are rapidly eliminated by the kidney and liver in contrast to negatively charged particles owing to their enhanced adsorption affinity to plasma protein [164,165]. However, the exact role of surface charge is not clear regarding the macrophage clearance of MNPs. Some studies showed that positively charged IONPs are more prone to liver uptake, but some showed that negative SPIONs are rapidly cleared via macrophage in contrast to non-ionic NPs [18]. It has been observed that one-dimensional NPs with a big length-to-width aspect ratio exhibited increased systemic circulation in contrast to spherical particles owing to their lower uptake by the macrophages. Elongated NPs having more probability to accumulate into the lymph nodes, while spherical accumulates preferably into the liver [18,162].

#### 6.1.3. Surface coating

Pure MNPs are structurally unstable, aggregated, and eliminated by RES resulting in a short half-life. Moreover, the aggregated form of MPNs clogs the blood vessels and reduced therapeutic potential. Therefore, MNPs should be properly stabilized via surface coating by an inert and biocompatible material that provides the core material protection, enhanced water solubility, reduction in drug-associated adverse reactions, targeted drug delivery, and extend the half-life of the drug by preventing opsonization by plasma proteins [1,37]. The nature of coating material significantly influences the particle size, pharmacokinetics, and biodistribution of the MNPs inside the body (Section. 4).

#### 6.1.4. Routes of administration

Various routes of administration like intravenous (*i.v.*), oral, nasal, and pulmonary significantly influence the MNPs pharmacokinetics. MNPs administered via the *i.v.* route are specifically taken up by the liver and spleen resulting in the blood clearance of MNPs via opsonization, followed by the identification via macrophages, and phagocytosis. Opsonization (plasma protein adsorption on the surface of MNPs) increases the size of MNPs leading to an increase in hepatic clearance [166]. Various parameters like type, charge, and functional groups of coating molecules regulate the composition and thickness of protein corona around the MNPs. Briefly, plasma protein adsorbs on the MNPs surface which is further recognized by macrophages and eliminated by the mononuclear phagocytic system (MPS) [162]. The MPS comprises blood circulating monocytes, and macrophages present on the liver, lung, spleen, bone marrow, brain, and lymph nodes [18]. However, when a large quantity is administered then the liver and spleen can only eliminate a small portion and an excess portion is accumulated into adipose tissues and lungs [167].

MNPs administered via the intrapulmonary or nasal route are mainly used for the treatment of pulmonary diseases and lung cancer [168]. Some studies revealed that IONPs are mainly accumulated ~2.5-fold in the central lung as compared to the peripheral lungs [169]. However, the macrophages located on the lung alveoli digest the MNPs through phagocytosis enabling restriction of the MNPs entry into the systemic circulation [18].

Orally administered MNPs usually accumulate to the gastrointestinal tract (GIT) and used for the treatment of

various GIT disorders and tumors. However, this route faces some problems like instability and poor bioavailability due to the presence of various enzymes and gastric acid [170]. MNPs coated with various surface coating agents (pKa ~3–5) can overcome the GI acidic environment and diffuses through the liver sinusoids before reaching the systemic circulation [162]. The stealthy behavior of coated MNPs can combat the liver phagocytosis enabling to increase in the half-life of the formulation. Recently,  $\beta$ -cyclodextrin-PEG-FA coated camptothecin-loaded MNPs exhibited enhanced antitumor activity [171]. Other routes such as intraperitoneal, intramuscular, retroorbital, and subcutaneous are also used for the administration of MNPs. However, more investigations are required to understand the pharmacokinetics and biodistribution of MNPs administered by these routes.

## 6.2. Evaluation of pharmacokinetic parameters and biodistribution

Various techniques like AC biosusceptometry (ACB) [172], spectroscopy, magnetometry [18,173], and imaging are used to quantify the MNPs concentration in systemic circulation and various organs.

AC biosusceptometry is used for real-time monitoring of MNPs in the systemic circulation [172]. Spectroscopy like inductively coupled plasma-mass spectrometry is used to quantify the plasma drug and MNPs concentration [174]. Various magnetometry techniques like superconducting quantum interference device (SQUID) electron paramagnetic resonance (EPR), magnetic susceptibility measurement (MSM), and ferromagnetic resonance spectroscopy (FMR), are used to portray the iron from MNPs or endogenous iron [18]. The imaging methods including transmission electron microscopy (TEM), optical microscopy, MRI, MPI, etc., are used to characterize the biodistribution pattern of MNPs in various tissues [173]. TEM can easily observe the MNPs distribution in the thin tissue section (0.02  $\mu\text{m}$ ) owing to its enhanced resolution and magnification [175]. Furthermore, TEM combined with energy-dispersive X-ray spectroscopy (EDX) is also used to determine the intracellular distribution of MNPs [129]. Optical microscopy is used to characterize the distribution of iron (from blood or IONPs) in various tissue/organ and histopathological analyses [53].

## 7. Toxicity of HP-MNPs

There are a lot of nanotechnology-based products in the development stage and at least 12 USFDA approved nanomedicines are in the market, still, toxicity is the most important concern. MNPs are intentionally designed to administer into the biological system so they should be part of human physiology. Iron (the main component of red blood cells) is easily transported, metabolized, and stored in the human system [160]. Iron oxide MNPs such as Feridex, Endorem, Ferumoxtran-10, etc., are used clinically due to their biocompatibility and non-toxicity in contrast to other heavy metal NPs [122,176]. Some recent studies evidenced the nontoxicity and biocompatibility of IONPs when administered in a relevant dose (up to 100 mg/kg) [177-179]. However, various

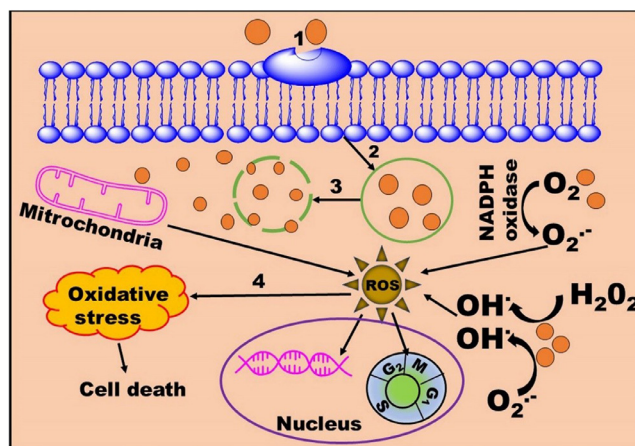


**Fig. 12 – Mechanism of MNPs toxicity. 1: Internalization of MNPs by endocytosis; 2: Generation of endocytic vesicles; 3: Lysozymatic degradation of MNPs and release of iron at pH~4.5; 4: Proteins/lipids oxidation.**

literature stipulated MNPs associated toxicity [16,160,176]. Therefore, MNPs associated toxicity needs to be addressed. In this section toxicity mechanism, factors affecting toxicity, and evaluation of toxicity will be discussed.

### 7.1. Mechanisms of toxicity

The MNPs mediated toxicity can be explained by the accumulation of MNPs inside the cell/tissues and the production of ROS [176]. ROS can be produced via Fenton/Haber-Weiss reaction [180] or direct production of ROS from the NPs surface [87]. Briefly, these accumulated MNPs especially iron-based MNPs are internalized by endocytosis and further degraded into iron by lysozymes at low pH (pH~4.5) [160,181]. The released iron is metabolized by RES and subsequently used by red blood cells or cleared by the kidney. An excess amount of iron can trigger ROS overproduction leading to adversely affects various activities like mitochondrial, nuclear, and cellular activity in combination or individually [159]. Moreover, various ROS such as hydroxyl ion, hydrogen peroxide, and oxygen radicals are also produced due to excess metal ion activators [108,122]. Further, ROS activates immune and anti-inflammatory mediators leading to induce oxidative stress. Moreover, ROS can deteriorate cell integrity or nuclear activity via protein denaturation, lipid peroxidation, DNA impairment, gene transcription modulation, damage signal transduction, leading to cell death (Fig. 12) [176].

### 7.2. Factors affecting toxicity

Toxicity is a complex phenomenon that mainly depends upon the intracellular localization of MNPs in various tissues/organs and interaction with the cytoskeleton [122]. Higher accumulation leads to increased interaction with the cytoskeleton resulting in cellular damage [159,182]. The degree of *in vitro* toxicity and ROS production is dependent upon the MNPs' physicochemical properties,



**Table 8 – In vitro toxicity of MNPs in different cell lines with different physicochemical properties and treatment conditions.**

Type of MNPs	Particle size	Dose concentration	Exposure time	Cell line	Toxicity	Ref
IONPs	15 nm & 225 nm	10–80 µg/ml		A549	No inherent toxicity	[196]
IONPs	72.6 nm	100, 800 and 1600 µg/ml	24 h	THP-1	Hemolysis	[197]
Sodium oleate coated IONPs & Silica coated IONPs	8 nm, 25 nm & 50 nm	0.12, 0.6, 3,15 and 75 µg/cm <sup>2</sup>	4, 24 or 48 h	BeWo b30 placental barrier	Cytotoxicity was dose and time dependent	[198]
Chitosan coated IONPs	6 nm & 8 nm	0.5, 2, 4 µg/µl	24, 48 and 72 h	HeLa, A549 and HeK293 cells	Chitosan coated IONPs was safer than the bare IONPs	[199]
Lipoamino Acid coated SPIONs	11 nm	1–500 µg/ml	24 and 48 h	Hep-G2	Bare SPION exhibited more toxicity in contrast to the coated SPION	[200]
Starch coated Fe <sub>3</sub> O <sub>4</sub> MNPs and dextran coated Fe <sub>3</sub> O <sub>4</sub> MNPs	100 nm	0.01–0.5 mg/ml	1 h–72 h	Rat pheochromocytoma PC12 cells	Bared MNPs exhibited magnified penetration without any toxicity. However, cellular uptake was dependent on the incubation time and MNPs concentration in the media.	[201]
Amino acid coated IONPs	3.98, 4.09, 3.41, 4.32, 2.35 nm	0.049, 0.073, 0.110, 0.165, 0.248 and 0.373 mg/ml	72 h	HFF2 cell lines	All the surface coated MNPs were biocompatible	[202]
Chitosan-dextran coated IONPs	55 nm	1, 5, 10, 50 and 150 µg/ml	1, 3, 12, and 24 h	Human cervix carcinoma HeLa cells	Dose and the time-dependent cytotoxic effect was observed	[203]

MNPs' chemical composition, protein corona, cell type, the biodegradability of MNPs, dose concentration, and exposure time (Table 8). Additionally, administered dose quantity, route of administration, surface coating, pharmacokinetics, and biodistribution also plays an important role in vivo toxicity (Table 9) [16,18,87,160]. Moreover, Age also influences iron toxicity due to different serum ferritin concentrations (male:15–320 mg/ml, and Female: 6–155 mg/ml).

MNPs physicochemical properties like particle size, surface area, shape, and surface coating play an important role in ROS generation. Particle size determines the transport, cellular interaction, and defense mechanism. Smaller NPs (1–100 nm) with larger surface area exhibited enhanced toxicity due to easy penetration through the cellular membrane enabling to increase in the NPs concentration [183,184]. However, some studies showed that no significant difference was observed due to size-dependent toxicity [185]. Rod shape IONPs showed more toxicity than spherical NPs due to more accumulation into the cytoplasm [186]. Surface coating is an important factor influencing the MNPs associated toxicity. Studies revealed that the coated MNPs are more biocompatible and nontoxic in contrast to bare MNPs due to lesser oxidative sites [16,36,122]. Additionally, bare NPs can induce the overproduction of ROS leading to alter cellular morphology and genotoxicity [181]. Various coating agents are used to increasing the stability and biocompatibility of MNPs (Section 4). However, some studies reported that carboxydextran and oleate-coated MNPs are more toxic as compared to bare MNPs. Thus, the composition of the coating

and thickness of the coating material should be properly selected for successful biomedical application.

Overproduction of ROS is associated with the MNPs' chemical composition and crystallinity [184]. It has been observed that at neutral pH higher ratio of Fe (II, III) can increase the ROS production [181]. Moreover, the oxidation state of Fe (magnetite and maghemite) and stoichiometric ratio of Fe<sup>2+</sup> and Fe<sup>3+</sup> also influence cellular toxicity. Studies revealed that magnetite exhibited more toxicity as compared to maghemite due to its oxidation [36,181]. Another study showed that same size TiO<sub>2</sub> NPs with prism-shaped crystal structure exhibited more cellular/nuclear toxicity as compared to the octahedral shaped NPs. However, the crystalline structure of NPs depends upon the dispersion medium, biological fluids composition [184]. Furthermore, the extent of toxicity also depends upon the cell type [181]. It has been observed that MNPs with similar physicochemical properties exhibited different toxicity in different cell lines [36,108,122]. This variation may be due to different contact points between the MNPs surface and cell membrane. Moreover, various studies demonstrated that the behavior of cell lines in 3-dimensional culture was similar to cell lines in vivo [176].

### 7.3. Evaluation of toxicity

Various techniques and assays are used to evaluate the in-vitro and in-vivo toxicity of MNPs (Table 10). In vitro assays such as proliferation, apoptosis, necrosis, oxidative

**Table 9 – In vivo toxicity of MNPs in various animal models using different routes of administration.**

Type of MNPs	Size	Animal	Route of administration	Dose/Time	Toxicity	Ref
Polyacrylic acid-coated cobalt ferrite MNPs	9.2 nm	Albino mice	i.m	100 µg/ml	No vital organ toxicity was observed	[204]
Aminocellulose, PAMAM dendrimers generation-2, and parabenpoly ethylene glycol coated IONPs	100–110 nm	Swiss albino mice (female)	i.v	5, 10 and 25 mg/kg	The triple layer coated MNPs were found biocompatible at all doses. Whereas, bare MNPs exhibited toxicity to vital organs at a higher dose	[205]
IONPs	15 nm & 225 nm	Balb/c mice (male)	s.c	2 × 10 <sup>6</sup> cells/100 µl PBS	No inherent toxicity	[196]
IONPs	72.6 nm	IGS rats (female)	i.v	12 mg/kg for 6 d	Eryptosis	[197]
IONPs	15 nm	Zebrafish	–	Incubated in a fish tank at 1 ppm and 10 ppm for 14 d	No behavioral toxicity was observed at 1 ppm but neurotoxicity was observed at 10 ppm	[206]
Polyethyleneimine-coated and poly(acrylic acid)-coated IONPs	28–30 nm	CrI:CD1(ICR) (CD-1) mice (male and female)	i.p	10 and 100 mg/kg on gestation day 8, 9 or 10	No toxicity was observed at 10 mg/kg regardless to charge. However, charge-dependent toxicity was observed at 100 mg/kg	[207]
Alendronic- and undecylenic acid-coated MNPs	21 nm	C57BL/6 mice (male)	i.v	0.5, 5, 50, and 500 µg/ml for 24 h 48 h	The coated MNPs exhibited dose-dependent cytotoxicity	[208]
PEI coated IONPs and PEG coated IONPs	10–30 nm	Nude mice (Nu/Nu strain) and BALB/c mice	i.v	1.5 mg/kg for biodistribution study and 1.5, 2.5, or 5 mg/kg for toxicity	No toxicity was observed for pegylated MNPs whereas, PEI-coated MNPs exhibited dose-dependent severe toxicity	[209]
Chitosan-dextran SPIONs	55 nm	Wistar rats (male)	i.v	2.5 mg/kg	The results revealed that the charged MNPs exhibited magnified cellular uptake enabling augmented cytotoxicity	[203]
Ferrite and manganese ferrite oxide MNPs	3–20 nm	Zebrafish embryos and Balb/c mice (male)	i.v	0.01, 0.1, 1, 10, 100 µg/ml	Normal hatching with no mortality was observed in the zebrafish model exposed to IONPs. However, manganese ferrite exhibited significant toxicity	[210]
Carbon coated MNPs	24 nm	Zebrafish	–	Incubated in a fish tank at 1 ppm and 10 ppm for 14 d	Carbon coated MNPs were safe as compared to the uncoated MNPs	[42]
PAMAM dendrimers generation-4 coated IONPs	241 nm	BALB/c mice	i.p	5 mg/ml	Accute toxicity was observed	[211]

stress are simple, easy, and cost-effective without using the animals [187]. These assays are used to analyze alteration in membrane integrity, nuclear and metabolic activities of cells after interaction with the MNPs. MTT ((3-(4,5-dimethylthiazol-2-yl)-2,5-diphenyltetrazolium bromide) or MTS ((3-(4,5-

dimethylthiazol-2-yl)-5-(3-carboxymethoxyphenyl)-2-(4-sulfophenyl)-2H-tetrazolium) assays are widely used to evaluate cytotoxicity studies by using different cell lines [181]. The result reproducibility depends upon the types of

**Table 10 – Various techniques and assays used to analyze MNPs associated toxicity [129,176,187].**

Technique/Assay	Parameter
Fluorescence microscopy	ROS, cytotoxicity, apoptosis
Flow cytometry	ROS, cytotoxicity, apoptosis, cell cycle impairment, cellular uptake
Spectrophotometric technique	Haemolysis, iron assay, quantification of NP uptake
Western blot	Cell cycle regulation, autophagy
SEM and TEM	Autophagosome formation, morphological changes in cell line
Single-cell electrophoresis	Genotoxicity, apoptosis
MTT	Cytotoxicity
Clonogenic assay	Cell survival
Comet assay	Genotoxicity, apoptosis
Annexin-V assay	Apoptosis
TUNEL	Apoptosis
Trypan blue exclusion assay	Stability of cell membrane
Amplex red assay	Oxidative stress
Nitro blue tetrazolium assay	Oxidative stress

cells, physicochemical properties of NPs, assay procedures, composition, and conditions of cell culture media [16,176,184].

Despite the reproducibility and cost-effectiveness of *in vitro* studies, poor correlation can be made between *in vitro* and *in vivo* studies [181]. This contradiction may be due to the complex microenvironment and homeostasis system of the human body [176]. *In vivo* studies are usually carried out in animal models for months or years due to prolonged systemic circulation. These studies are useful for a better understanding of absorption, distribution, metabolism, excretion, and toxicity of MNPs in the living organism [159]. Various animal models like murine [188], zebrafish [189], and rabbit [144] are used to evaluate the changes in serum chemistry, organ histopathology, and genetic profiles [18,187].

Furthermore, various spectrophotometric (ICPMS, Prussian blue staining, ferozoin, quantichrom assay, and imaging techniques (Section 5.2.3) are used to quantify the uptake of NPs inside the body [181].

## 8. Challenges and future perspectives

Although significant technological progress has been made regarding biocompatible MNPs synthesis, characterization, and post-synthetic modification for efficient biomedical applications yet few MNPs based formulations are under clinical trials due to some challenges [87]. Therefore, some critical points need to be researched further to overcome certain challenges like crossing the biological barriers, MDT/MH therapy, recognizing the interaction of MNPs with the complex human biological environment, escaping the immune system, and MNPs associated toxicity.

After administration, all the formulations including MNPs face various biological barriers that diminish the localization or site-specific targeting resulting in the poor therapeutic efficacy of the formulation. Moreover, nonspecific distribution, drug efflux pumps, opsonization, MPS clearance, endosomal escape, and cellular internalization also mitigate the therapeutic efficacy of MNPs. These limitations can

be overcome by modulating the size, shape, surface chemistry, composition, drug loading, pharmacokinetics, and biodistribution of the MNPs. Therefore, smaller size MNPs with augmented magnetic sensitivity should be fabricated to maintain the magnified spatial and temporal responsiveness. Mostly reported MNPs are either spherical in the shape or possess a low aspect ratio. Further shape variations of these nanocarriers and magnetically actuated nanomedicines can be superparamagnetic nanotube, nanorods, nanodiscs, nano worms, and nano chains, etc. These MNPs can be explored in combination with other heterostructure composites with improved properties for drug loading and deep signal collections. A new class of materials like MMOF, MLs, cobalt-based magnetic carbons, etc. can be among candidate molecules for these synergies.

MDT in humans is another challenge due to thick skin and tissues in comparison to other test models. Moreover, the absence of homogeneous penetration of MNPs also hinders the therapeutic efficiency of the drug delivery system. Current targeting is restricted to the superficial area as the magnetic field for deeper application is not sufficient and needs to be improved and optimized for efficient MDT [161]. Additionally, targeting specific organs /tissues especially tumors is another challenge owing to their complex structure [64]. Various strategies like conjugation of antibodies, specific ligands, immunomodulators have been used to magnify the targeting but <10% MNPs are successful for prolonged delivery with minimum toxicity [87].

As per the literature, the maximum frequency and amplitude are  $H \times f < 5 \times 10^9$ , but the exposure effect of AMF in various tissues and organs has not been properly investigated in MH therapy. Recently, various studies revealed that variation in a magnetic field such as amplitude and frequency [100], speed, and direction [101], influences the MH efficiency. More research should be carried out to explore other factors which affect eddy heating in various tissues or organs [64].

Furthermore, extensive safety and toxicity data requirement is another challenge for the regulatory approval in human application. Although, a lot of data is available on

the toxicity of these MNPs in terms of purity, functionality, and geometrical isotropy yet the research must be going on in the future to explain the impact of particles on chemical and physical asymmetry in an in-vivo environment. Chemical (functional group) diversity, amphiphilicity, high dipole moments, and shape anisotropy are further concerns in-vivo usage [17]. Therefore, a multidisciplinary collaboration should be taken between the various research/academic institutions and regulatory authorities.

## 9. Conclusion

MNPs have manifested high potential applications in various research and industrial communities like physics, chemistry, electronics, environmental, and healthcare owing to their unique properties. Biomedically, MNPs are designed to accomplish prolonged site-specific drug delivery, diagnostic, and imaging without any adverse effects. Therefore, various physicochemical properties like particle size, surface charge, hydrophobicity, and shape should be modulated for the successful transportation of MNPs through the biological membrane by escaping the immune system. Moreover, the synthesis method also governs the post-synthetic modification and specific applications. However, MNPs face certain limitations such as loss of magnetic property, oxidation, aggregation, and poor storage stability. These limitations can be overcome by stabilization of MNPs by using suitable coating materials such as inorganic and organic biocompatible materials like polymers, metal, metal oxides, silica, etc.

Despite their extensive use in the health care system few formulations are under clinical trials/clinically used due to certain challenges like toxicity, long-term effectiveness, physiological pH stability, and specific targeting to the deeply located large blood vessels. Moreover, some pharmacokinetic alterations in the parent therapeutic modalities also may lead to toxic/side effects. Therefore, the *in vivo* fate of MNPs needs to be addressed to figure out the biological behavior, interaction with the living organism, and efficacy. The pharmacokinetics and biodistribution of MNPs are significantly influenced by various factors like physicochemical properties and surface functionalization of MNPs. Additionally, routes of administration, biological fluid composition, and opsonization also affect the various pharmacokinetic parameters like plasma half-life ( $T_{1/2}$ ), distribution, and elimination.

The clinical use of MNPs may be increased by magnifying their loading capacity, improving pharmacokinetic and biodistribution parameters with increased therapeutic efficacy and specificity to the target site without any toxic effects. These can be improved by post-synthetic modification or fabrication of various organic-inorganic biocompatible magnetic micro/nanocomposites like magnetoliposomes, magnetic microrobots, stimuli-responsive magnetic nanosystem, stimuli-responsive magnetic nanomicelles, and ultramagnetic liposomes and magnetic metal-organic frameworks, etc. Post synthetic modification comprises functionalization/loading of various components onto the surface or inside the core of MNPs resulting in HP-

MNPs. Further, the therapeutic efficacy of HP-MNPs can also be synergized by combining with other therapies like chemotherapy, radiotherapy, immunotherapy, photodynamic therapy, and gene therapy. The synthesis of HP-MNPs with reduced dosage and minimum adverse effects is still in progress. Additionally, the tailored properties of HP-MNPs and customization options in detection techniques open new possibilities for new detection combinations. Although considerable efforts have been made to improve the clinical application of MNPs, more multidisciplinary collaborative research must be required to completely overcome the long-term toxicity.

## Conflicts of interest

The authors declare no conflicts of interest.

## Acknowledgement

Parveen Kumar acknowledges the department of science and technology (DST), New Delhi for the INSPIRE (Innovation in Science Pursuit for Inspired Research)-Faculty grant.

## REFERENCES

- [1] Mosayebi J, Kiyasatfar M, Laurent S. Synthesis, functionalization, and design of magnetic nanoparticles for theranostic applications. *Adv Healthc Mater* 2017;6(23):1700306.
- [2] Tartaj P, Morales MP, Veintemillas VS, Gonzalez CT, Serna CJ. The preparation of magnetic nanoparticles for applications in biomedicine. *J Phys D Appl Phys* 2003;36(13):182–97.
- [3] Tran N, Webster TJ. Magnetic nanoparticles: biomedical applications and challenges. *J Mater Chem* 2010;20(40):8760–7.
- [4] Cardoso VF, Francesco A, Ribeiro C, Bañobre-López M, Martins P, Lancersos-Mendez S. Advances in magnetic nanoparticles for biomedical applications. *Adv Healthc Mater* 2018;7(5):1700845.
- [5] Biehl P, Von der Lühe M, Dutz S, Schacher FH. Synthesis, characterization, and applications of magnetic nanoparticles featuring polyzwitterionic coatings. *Polymers (Basel)* 2018;10(1):91.
- [6] Mohammed L, Gomaa HG, Ragab D, Zhu J. Magnetic nanoparticles for environmental and biomedical applications: a review. *Particuology* 2017;30:1–14.
- [7] Zhu N, Ji H, Yu P, Niu J, Farooq MU, Akram MW, et al. Surface modification of magnetic iron oxide nanoparticles. *Nanomaterials (Basel)* 2018;8(10):810.
- [8] Li X, Zhang XN, Li XD, Chang J. Multimodality imaging in nanomedicine and nanotheranostics. *Cancer Biol Med* 2016;13(3):339–48.
- [9] Reddy LH, Arias JL, Nicolas J, Couvreur P. Magnetic nanoparticles: design and characterization, toxicity and biocompatibility, pharmaceutical and biomedical applications. *Chem Rev* 2012;112(11):5818–78.
- [10] Ali A, Zafar H, Zia M, Ul Haq I, Phull AR, Ali JS, et al. Synthesis, characterization, applications, and challenges of iron oxide nanoparticles. *Nanotechnol Sci Appl* 2016;9:49–67.

- [11] Kempe H, Kates SA, Kempe M. Nanomedicine's promising therapy: magnetic drug targeting. *Expert Rev Med Devices* 2011;8(3):291–4.
- [12] Li X, Wei J, Aifantis KE, Fan Y, Feng Q, Cui FZ, et al. Current investigations into magnetic nanoparticles for biomedical applications. *J Biomed Mater Res A* 2016;104(5):1285–96.
- [13] Mahmoudi M, Sant S, Wang B, Laurent S, Sen T. Superparamagnetic iron oxide nanoparticles (spions): development, surface modification and applications in chemotherapy. *Adv Drug Deliv Rev* 2011;63(1–2):24–46.
- [14] Savla R, Garbuzenko OB, Chen S, Rodriguez-Rodriguez L, Minko T. Tumor-targeted responsive nanoparticle-based systems for magnetic resonance imaging and therapy. *Pharm Res* 2014;31(12):3487–502.
- [15] Hedayatnasab Z, Abnisa F, Daud WMAW. Review on magnetic nanoparticles for magnetic nanofluid hyperthermia application. *Mater Des* 2017;123:174–96.
- [16] Arias LS, Pessan JP, Vieira APM, TMTd Lima, Delbem ACB, Monteiro DR. Iron oxide nanoparticles for biomedical applications: a perspective on synthesis, drugs, antimicrobial activity, and toxicity. *Antibiotics (Basel)* 2018;7(2):46.
- [17] Hosu O, Tertis M, Cristea C. Implication of magnetic nanoparticles in cancer detection, screening and treatment. *Magnetochemistry* 2019;5(4):55.
- [18] Arami H, Khandhar A, Liggitt D, Krishnan KM. *In vivo* delivery, pharmacokinetics, biodistribution and toxicity of iron oxide nanoparticles. *Chem Soc Rev* 2015;44(23):8576–607.
- [19] Martínez-Cabanas M, López-García M, Barriada JL, Herrero R, Sastre de Vicente ME. Green synthesis of iron oxide nanoparticles. Development of magnetic hybrid materials for efficient as(v) removal. *Chem Eng J* 2016;301:83–91.
- [20] Liu Y, Yang J, Xie M, Xu J, Li Y, Shen H, et al. Synthesis of polyethyleneimine-modified magnetic iron oxide nanoparticles without adding base and other additives. *Mater Lett* 2017;193:122–5.
- [21] Rajiv P, Bavadarani B, Kumar MN, Vanathi P. Synthesis and characterization of biogenic iron oxide nanoparticles using green chemistry approach and evaluating their biological activities. *Biocatal Agric Biotechnol* 2017;12:45–9.
- [22] Gul S, Khan SB, Rehman IU, Khan MA, Khan MI. A comprehensive review of magnetic nanomaterials modern day theranostics. *Front Mater* 2019;6:179.
- [23] Lu M, Ozcelik A, Grigsby CL, Zhao Y, Guo F, Leong KW, et al. Microfluidic hydrodynamic focusing for synthesis of nanomaterials. *Nano Today* 2016;11(6):778–92.
- [24] Surowiec Z, Budzyński M, Durak K, Czernel G. Synthesis and characterization of iron oxide magnetic nanoparticles. *Nukleonika* 2017;62(2):73.
- [25] Freitas JCD, Branco RM, Lisboa IGO, Costa TPD, Campos MGN, Jafellicci JM, et al. Magnetic nanoparticles obtained by homogeneous coprecipitation sonochemically assisted. *Mater Res* 2015;18:220–4.
- [26] Laurent S, Forge D, Port M, Roch A, Robic C, Vander Elst L, et al. Magnetic iron oxide nanoparticles: synthesis, stabilization, vectorization, physicochemical characterizations, and biological applications. *Chem Rev* 2008;108(6):2064–110.
- [27] Hufschmid R, Arami H, Ferguson RM, Gonzales M, Teeman E, Brush LN, et al. Synthesis of phase-pure and monodisperse iron oxide nanoparticles by thermal decomposition. *Nanoscale* 2015;7(25):11142–54.
- [28] Patsula V, Kosinová L, Lovrić M, Ferhatovic Hamzić L, Rabyk M, Konefal R, et al. Superparamagnetic Fe<sub>3</sub>O<sub>4</sub> nanoparticles: synthesis by thermal decomposition of iron(iii) glucuronate and application in magnetic resonance imaging. *ACS Appl Mater Interfaces* 2016;8(11):7238–47.
- [29] Huber DL. Synthesis, properties, and applications of iron nanoparticles. *Small* 2005;1(5):482–501.
- [30] Berlan J. Microwaves in chemistry: another way of heating reaction mixtures. *Radiat Phy Chem* 1995;45(4):581–9.
- [31] Deshmukh R, Niederberger M. Mechanistic aspects in the formation, growth and surface functionalization of metal oxide nanoparticles in organic solvents. *Chemistry (Easton)* 2017;23(36):8542–70.
- [32] Watt J, Bleier GC, Austin MJ, Ivanov SA, Huber DL. Non-volatile iron carbonyls as versatile precursors for the synthesis of iron-containing nanoparticles. *Nanoscale* 2017;9(20):6632–7.
- [33] de Toledo LAS, Rosseto HC, Bruschi ML. Iron oxide magnetic nanoparticles as antimicrobials for therapeutics. *Pharm Dev Technol* 2018;23(4):316–23.
- [34] Zhao H, Liu R, Zhang Q, Wang Q. Effect of surfactant amount on the morphology and magnetic properties of monodisperse ZnFe<sub>2</sub>O<sub>4</sub> nanoparticles. *Mater Res Bull* 2016;75:172–7.
- [35] Shabestari KS, Farshbaf M, Akbarzadeh A, Davaran S. Magnetic nanoparticles: preparation methods, applications in cancer diagnosis and cancer therapy. *Artif Cells Nanomed Biotechnol* 2017;45(1):6–17.
- [36] Schladt TD, Schneider K, Schild H, Tremel W. Synthesis and bio-functionalization of magnetic nanoparticles for medical diagnosis and treatment. *Dalton Trans* 2011;40(24):6315–43.
- [37] Albinali KE, Zagho MM, Deng Y, Elzatahry AA. A perspective on magnetic core-shell carriers for responsive and targeted drug delivery systems. *Int J Nanomed* 2019;14:1707–23.
- [38] Kumar R, Mondal K, Panda PK, Kaushik A, Abolhassani R, Ahuja R, et al. Core-shell nanostructures: perspectives towards drug delivery applications. *J Mater Chem B* 2020;8(39):8992–9027.
- [39] Fang C, Zhang M. Multifunctional magnetic nanoparticles for medical imaging applications. *J Mater Chem* 2009;19(35):6258–66.
- [40] Lu AH, Salabas EL, Schüth F. Magnetic nanoparticles: synthesis, protection, functionalization, and application. *Angew Chem Int Ed Engl* 2007;46(8):1222–44.
- [41] Lai H, Xu F, Wang L. A review of the preparation and application of magnetic nanoparticles for surface-enhanced raman scattering. *J Mater Sci* 2018;53(12):8677–98.
- [42] Malhotra N, Audira G, Chen JR, Siregar P, Hsu HS, Lee JS, et al. Surface modification of magnetic nanoparticles by carbon-coating can increase its biosafety: evidences from biochemical and neurobehavioral tests in zebrafish. *Molecules (Basel)* 2020;25(9):2256.
- [43] Liu Y, Li M, Yang F, Gu N. Magnetic drug delivery systems. *Sci China Mater* 2017;60(6):471–86.
- [44] Anderson SD, Gwenin VV, Gwenin CD. Magnetic functionalized nanoparticles for biomedical, drug delivery and imaging applications. *Nanoscale Res Lett* 2019;14(1):188.
- [45] Jayant RD, Tiwari S, Atluri V, Kaushik A, Tomitaka A, Yndart A, et al. Multifunctional nanotherapeutics for the treatment of neuroaids in drug abusers. *Sci Rep* 2018;8(1):12991.
- [46] Connell JJ, Patrick PS, Yu Y, Lythgoe MF, Kalber TL. Advanced cell therapies: targeting, tracking and actuation of cells with magnetic particles. *Regen Med* 2015;10(6):757–72.
- [47] Price PM, Mahmoud WE, Al-Ghamdi AA, Bronstein LM. Magnetic drug delivery: where the field is going. *Front Chem* 2018;6:619.
- [48] Riegler J, Liew A, Hynes SO, Ortega D, O'Brien T, Day RM, et al. Superparamagnetic iron oxide nanoparticle

- targeting of MSCs in vascular injury. *Biomaterials* 2013;34(8):1987–94.
- [49] Al-Jamal KT, Bai J, Wang JT, Protti A, Southern P, Bogart L, et al. Magnetic drug targeting: preclinical *in vivo* studies, mathematical modeling, and extrapolation to humans. *Nano Lett* 2016;16(9):5652–60.
- [50] Reczyńska K, Marszałek M, Zarzycki A, Reczyński W, Kornaus K, Pamuła E, et al. Superparamagnetic iron oxide nanoparticles modified with silica layers as potential agents for lung cancer treatment. *Nanomaterials (Basel)* 2020;10(6):1076.
- [51] Cardoso VF, Francesko A, Ribeiro C, Bañobre-López M, Martins P, Lanceros-Mendez S. Advances in magnetic nanoparticles for biomedical applications. *Adv Health Mater* 2018;7(5):1700845.
- [52] Cai M, Chen G, Qin L, Qu C, Dong X, Ni J, et al. Metal organic frameworks as drug targeting delivery vehicles in the treatment of cancer. *Pharmaceutics* 2020;12(3):232.
- [53] Kush P, Kaur M, Sharma M, Madan J, Kumar P, Deep A, et al. Investigations of potent biocompatible metal-organic framework for efficient encapsulation and delivery of gemcitabine: biodistribution, pharmacokinetic and cytotoxicity study. *Biomed Phys Eng Express* 2020;6(2):025014.
- [54] Szuplewska A, Rękorajska JA, Pocztańska E, Krysiński P, Dybko A, Chudy M. Magnetic field-assisted selective delivery of doxorubicin to cancer cells using magnetoliposomes as drug nanocarriers. *Nanotechnology* 2019;30(31):315101.
- [55] Guo Y, Zhang Y, Ma J, Li Q, Li Y, Zhou X, et al. Light/magnetic hyperthermia triggered drug released from multi-functional thermo-sensitive magnetoliposomes for precise cancer synergetic theranostics. *J Control Rel* 2018;272:145–58.
- [56] Sitti M. Miniature soft robots -road to the clinic. *Nat Rev Mater* 2018;3(6):74–5.
- [57] Kim DI, Lee H, Kwon SH, Choi H, Park S. Magnetic nano-particles retrievable biodegradable hydrogel microrobot. *Sens Actuators B Chem* 2019;289:65–77.
- [58] Mai BT, Fernandes S, Balakrishnan PB, Pellegrino T. Nanosystems based on magnetic nanoparticles and thermo- or ph-responsive polymers: an update and future perspectives. *Acc Chem Res* 2018;51(5):999–1013.
- [59] Ghamkhari A, Ghorbani M, Aghbolaghi S. A perfect stimuli-responsive magnetic nanocomposite for intracellular delivery of doxorubicin. *Artif Cells Nanomed Biotechnol* 2018;46(sup3):911–21.
- [60] Malaekhepoor SM, Derakhshandeh K, Haddadi R, Nourian A, Ghorbani-Vaghei R. A polymer coated MNP scaffold for targeted drug delivery and improvement of rheumatoid arthritis. *Polym Chem* 2020;11(13):2408–17.
- [61] Yang J, Wang Y, Pan M, Xie X, Liu K, Hong L, et al. Synthesis of magnetic metal-organic frame material and its application in food sample preparation. *Foods* 2020;9(11):1610.
- [62] Hashemipour S, Ahmad Panahi H. Fabrication of magnetite nanoparticles modified with copper based metal organic framework for drug delivery system of letrozole. *J Mol Liq* 2017;243:102–7.
- [63] Pinna A, Ricco R, Migheli R, Rocchitta G, Serra PA, Falcaro P, et al. A MOF-based carrier for *in situ* dopamine delivery. *RSC Adv* 2018;8(45):25664–72.
- [64] Liu X, Zhang Y, Wang Y, Zhu W, Li G, Ma X, et al. Comprehensive understanding of magnetic hyperthermia for improving antitumor therapeutic efficacy. *Theranostics* 2020;10(8):3793–815.
- [65] Noh SH, Na W, Jang JT, Lee JH, Lee EJ, Moon SH, et al. Nanoscale magnetism control via surface and exchange anisotropy for optimized ferrimagnetic hysteresis. *Nano Lett* 2012;12(7):3716–21.
- [66] Serantes D, Simeonidis K, Angelakeris M, Chubykalo FO, Marciello M, Morales MP, et al. Multiplying magnetic hyperthermia response by nanoparticle assembling. *J Phy Chem C* 2014;118(11):5927–34.
- [67] Piazza RD, Viali WR, dos Santos CC, Nunes ES, Marques RFC, Morais PC, et al. Peglatyon-SPION surface functionalization with folic acid for magnetic hyperthermia applications. *Mater Res Express* 2020;7(1):015078.
- [68] Piehler S, Dähring H, Grandke J, Göring J, Couleaud P, Aires A, et al. Iron oxide nanoparticles as carriers for Dox and magnetic hyperthermia after intratumoral application into breast cancer in mice: impact and future perspectives. *Nanomaterials (Basel)* 2020;10(6):1016.
- [69] Kim DH, Vitol EA, Liu J, Balasubramanian S, Gosztola DJ, Cohen EE, et al. Stimuli-responsive magnetic nanomicelles as multifunctional heat and cargo delivery vehicles. *Langmuir* 2013;29(24):7425–32.
- [70] Wang Q, Xiao J, Su Y, Huang J, Li J, Qiu L, et al. Fabrication of thermoresponsive magnetic micelles from amphiphilic poly(phenyl isocyanide) and Fe<sub>3</sub>O<sub>4</sub> nanoparticles for controlled drug release and synergistic thermochemotherapy. *Polym Chem* 2021;12(14):2132–40.
- [71] Béalle G, Di Corato R, Kolosnjaj-Tabi J, Dupuis V, Clément O, Gazeau F, et al. Ultra magnetic liposomes for MR imaging, targeting, and hyperthermia. *Langmuir* 2012;28(32):11834–42.
- [72] Jabalera Y, Fernández-Vivas A, Iglesias GR, Delgado ÁV, Jimenez-Lopez C. Magnetoliposomes of mixed biomimetic and inorganic magnetic nanoparticles as enhanced hyperthermia agents. *Colloids Surf B: Biointerfaces* 2019;183:110435.
- [73] Kumar R, Chauhan A, Jha SK, Kuanr BK. Localized cancer treatment by radio-frequency hyperthermia using magnetic nanoparticles immobilized on graphene oxide: from novel synthesis to *in vitro* studies. *J Mater Chem B* 2018;6(33):5385–99.
- [74] Sugumaran PJ, Liu XL, Herng TS, Peng E, Ding J. GO-functionalized large magnetic iron oxide nanoparticles with enhanced colloidal stability and hyperthermia performance. *ACS Appl Mater Interfaces* 2019;11(25):22703–13.
- [75] Asgari M, Miri T, Soleymani M, Barati A. A novel method for *in situ* encapsulation of curcumin in magnetite-silica core-shell nanocomposites: a multifunctional platform for controlled drug delivery and magnetic hyperthermia therapy. *J Mol Liq* 2021;324:114731.
- [76] Santha Moorthy M, Subramanian B, Panchanathan M, Mondal S, Kim H, Lee KD, et al. Fucoidan-coated core-shell magnetic mesoporous silica nanoparticles for chemotherapy and magnetic hyperthermia-based thermal therapy applications. *New J Chem* 2017;41(24):15334–46.
- [77] Chen J, Liu J, Hu Y, Tian Z, Zhu Y. Metal-organic framework-coated magnetite nanoparticles for synergistic magnetic hyperthermia and chemotherapy with pH-triggered drug release. *Sci Technol Adv Mater* 2019;20(1):1043–54.
- [78] Ren MX, Wang YQ, Lei BY, Yang XX, Hou YL, Meng WJ, et al. Magnetite nanoparticles anchored on graphene oxide loaded with doxorubicin hydrochloride for magnetic hyperthermia therapy. *Ceram Int* 2021;47(14):20686–92.
- [79] Gandia D, Gandarias L, Rodrigo I, Robles-García J, Das R, Garaió E, et al. Unlocking the potential of magnetotactic bacteria as magnetic hyperthermia agents. *Small* 2019;15(41):1902626.
- [80] Shuai C, Yang W, He C, Peng S, Gao C, Yang Y, et al. A

- magnetic micro-environment in scaffolds for stimulating bone regeneration. *Mater Des* 2020;185:108275.
- [81] Govindan R, Karthi S, Kumar GS, Girija EK. Development of Fe<sub>3</sub>O<sub>4</sub> integrated polymer/phosphate glass composite scaffolds for bone tissue engineering. *Mater Adv* 2020;1:3466–75.
- [82] Xia Y, Sun J, Zhao L, Zhang F, Liang XJ, Guo Y, et al. Magnetic field and nano-scaffolds with stem cells to enhance bone regeneration. *Biomaterials* 2018;183:151–70.
- [83] Rotherham M, Henstock JR, Qutachi O, El Haj AJ. Remote regulation of magnetic particle targeted wnt signaling for bone tissue engineering. *Nanomedicine* 2018;14(1):173–84.
- [84] Yamamoto Y, Ito A, Fujita H, Nagamori E, Kawabe Y, Kamihira M. Functional evaluation of artificial skeletal muscle tissue constructs fabricated by a magnetic force-based tissue engineering technique. *Tissue Eng Part A* 2011;17(1–2):107–14.
- [85] Mushtaq F, Torlakcik H, Vallmajo-Martin Q, Siringil EC, Zhang J, Röhrig C, et al. Magnetolectric 3D scaffolds for enhanced bone cell proliferation. *Appl Mater Today* 2019;16:290–300.
- [86] Fernandes MM, Correia DM, Ribeiro C, Castro N, Correia V, Lanceros-Mendez S. Bioinspired three-dimensional magnetoactive scaffolds for bone tissue engineering. *ACS Appl Mater Interfaces* 2019;11(48):45265–75.
- [87] Mukherjee S, Liang L, Veisoh O. Recent advancements of magnetic nanomaterials in cancer therapy. *Pharmaceutics* 2020;12(2):147.
- [88] Hong EJ, Choi DG, Shim MS. Targeted and effective photodynamic therapy for cancer using functionalized nanomaterials. *Acta Pharm Sin B* 2016;6(4):297–307.
- [89] Kwon YM, Je JY, Cha SH, Oh Y, Cho WH. Synergistic combination of chemo-phototherapy based on temozolomide/ICG-loaded iron oxide nanoparticles for brain cancer treatment. *Oncol Rep* 2019;42(5):1709–24.
- [90] Basoglu H, Bilgin MD, Demir MM. Protoporphyrin IX-loaded magnetoliposomes as a potential drug delivery system for photodynamic therapy: fabrication, characterization and in vitro study. *Photodiagn Photodyn Ther* 2016;13:81–90.
- [91] Choi KH, Nam KC, Cho G, Jung JS, Park BJ. Enhanced photodynamic anticancer activities of multifunctional magnetic nanoparticles (Fe<sub>3</sub>O<sub>4</sub>) conjugated with Chlorin e6 and folic acid in prostate and breast cancer cells. *Nanomaterials (Basel)* 2018;8(9):722.
- [92] Hou H, Huang X, Wei G, Xu F, Wang Y, Zhou S. Fenton reaction-assisted photodynamic therapy for cancer with multifunctional magnetic nanoparticles. *ACS Appl Mater Interfaces* 2019;11(33):29579–92.
- [93] Makola LC, Mgidlana S, Nyokong T. Amphiphilic axially modified cationic indium-porphyrins linked to hydrophilic magnetic nanoparticles for photodynamic antimicrobial chemotherapy against gram-negative strain; *Escherichia coli*. *Dyes Pigm* 2021;192:109262.
- [94] Ostroverkhov P, Semkina A, Naumenko V, Plotnikova E, Yakubovskaya R, Vodopyanov S, et al. HSA-coated magnetic nanoparticles for MRI-guided photodynamic cancer therapy. *Pharmaceutics* 2018;10(4):284.
- [95] Peltek OO, Muslimov AR, Zyuzin MV, Timin AS. Current outlook on radionuclide delivery systems: from design consideration to translation into clinics. *J Nanobiotechnol* 2019;17(1):90.
- [96] Munaweera I, Shi Y, Koneru B, Saez R, Aliev A, Di Pasqua AJ, et al. Chemoradiotherapeutic magnetic nanoparticles for targeted treatment of nonsmall cell lung cancer. *Mol Pharm* 2015;12(10):3588–96.
- [97] Zhu J, Zhang B, Tian J, Wang J, Chong Y, Wang X, et al. Synthesis of heterodimer radionuclide nanoparticles for magnetic resonance and single-photon emission computed tomography dual-modality imaging. *Nanoscale* 2015;7(8):3392–5.
- [98] Cędrowska E, Pruszyński M, Gawęda W, Żuk M, Krysiński P, Bruchertseifer F, et al. Trastuzumab conjugated superparamagnetic iron oxide nanoparticles labeled with <sup>225</sup>Ac as a perspective tool for combined  $\alpha$ -radioimmunotherapy and magnetic hyperthermia of HER2-positive breast cancer. *Molecules* 2020;25(5):1025.
- [99] Gawęda W, Pruszyński M, Cędrowska E, Rodak M, Majkowska-Pilip A, Gawęł D, et al. Trastuzumab modified barium ferrite magnetic nanoparticles labeled with Radium-223: a new potential radiobioconjugate for alpha radioimmunotherapy. *Nanomaterials (Basel)* 2020;10(10):2067.
- [100] Fouriki A, Clements MA, Farrow N, Dobson J. Efficient transfection of MG-63 osteoblasts using magnetic nanoparticles and oscillating magnetic fields. *J Tissue Eng Regen Med* 2014;8(3):169–75.
- [101] Oral O, Cıkım T, Zuvin M, Unal O, Yagci-Acar H, Gozuacik D, et al. Effect of varying magnetic fields on targeted gene delivery of nucleic acid-based molecules. *Ann Biomed Eng* 2015;43(11):2816–26.
- [102] Zuvin M, Kuruoglu E, Kaya VO, Unal O, Kutlu O, Yagci Acar H, et al. Magnetofection of green fluorescent protein encoding DNA-bearing polyethyleneimine-coated superparamagnetic iron oxide nanoparticles to human breast cancer cells. *ACS Omega* 2019;4(7):12366–74.
- [103] Cen C, Wu J, Zhang Y, Luo C, Xie L, Zhang X, et al. Improving magnetofection of magnetic polyethyleneimine nanoparticles into MG-63 osteoblasts using a novel uniform magnetic field. *Nanoscale Res Lett* 2019;14(1):90.
- [104] Blokpoel Ferreras LA, Chan SY, Vazquez Reina S, Dixon JE. Rapidly transducing and spatially localized magnetofection using peptide-mediated non-viral gene delivery based on iron oxide nanoparticles. *ACS Appl Nano Mater* 2021;4(1):167–81.
- [105] Singh A, Sahoo SK. Magnetic nanoparticles: a novel platform for cancer theranostics. *Drug Discov Today* 2014;19(4):474–81. doi:10.1016/j.drudis.2013.10.005.
- [106] Li J, Feng Z, Gu N, Yang F. Superparamagnetic iron oxide nanoparticles assembled magnetic nanobubbles and their application for neural stem cells labeling. *J Mater Sci & Technol* 2021;63:124–32.
- [107] Kim KY, Chang KA. Therapeutic potential of magnetic nanoparticle-based human adipose-derived stem cells in a mouse model of parkinson's disease. *Int J Mol Sci* 2021;22(2):654.
- [108] Shabatina TI, Vernaya OI, Shabatin VP, Melnikov MY. Magnetic nanoparticles for biomedical purposes: modern trends and prospects. *Magnetochemistry* 2020;6(3):30.
- [109] Fatima H, Kim K-S. Magnetic nanoparticles for bioseparation. *Korean J of Chem Eng* 2017;34(3):589–99.
- [110] Gloag L, Mehdipour M, Chen D, Tilley RD, Gooding JJ. Advances in the application of magnetic nanoparticles for sensing. *Adv Mater* 2019;31(48):1904385.
- [111] Fahmy SA, Alawak M, Brüßler J, Bakowsky U, El Sayed MMH. Nanoenabled bioseparations: current developments and future prospects. *BioMed Res Int* 2019;2019:4983291.
- [112] Zhou Y, Yan D, Yuan S, Chen Y, Fletcher EE, Shi H, et al. Selective binding, magnetic separation and purification of histidine-tagged protein using biopolymer magnetic core-shell nanoparticles. *Protein Expr Purif* 2018;144:5–11.
- [113] Zeng K, Sun EJ, Liu ZW, Guo J, Yuan C, Yang Y, et al. Synthesis of magnetic nanoparticles with an IDA or TED modified surface for purification and immobilization of poly-histidine tagged proteins. *RSC Adv* 2020;10(19):11524–34.
- [114] Minkner R, Xu J, Takemura K, Boonyakida J, Wätzig H,

- Park EY. Ni-modified magnetic nanoparticles for affinity purification of His-tagged proteins from the complex matrix of the silkworm fat body. *J Nanobiotechnology* 2020;18(1):159.
- [115] Rocha-Santos TAP. Sensors and biosensors based on magnetic nanoparticles. *Trends Analyt Chem* 2014;62:28–36.
- [116] Vallabani NVS, Singh S, Karakoti AS. Magnetic nanoparticles: current trends and future aspects in diagnostics and nanomedicine. *Curr Drug Metab* 2019;20(6):457–72.
- [117] Kalyani T, Sangili A, Nanda A, Prakash S, Kaushik A, Kumar Jana S. Bio-nanocomposite based highly sensitive and label-free electrochemical immunosensor for endometriosis diagnostics application. *Bioelectrochemistry* 2021;139:107740.
- [118] Kaushik A, Solanki PR, Ansari AA, Ahmad S, Malhotra BD. Chitosan-iron oxide nanobiocomposite based immunosensor for ochratoxin-A. *Electrochem Commun* 2008;10(9):1364–8.
- [119] Adem S, Jain S, Sveiven M, Zhou X, O'Donoghue AJ, Hall DA. Giant magnetoresistive biosensors for real-time quantitative detection of protease activity. *Sci Rep* 2020;10(1):7941.
- [120] Togawa K, Sanbonsugi H, Sandhu A, Abe M, Narimatsu H, Nishio K, et al. High sensitivity InSb hall effect biosensor platform for DNA detection and biomolecular recognition using functionalized magnetic nanobeads. *Jpn J Appl Phys* 2005;44(49):1494–7.
- [121] Farzin A, Etesami SA, Quint J, Memic A, Tamayol A. Magnetic nanoparticles in cancer therapy and diagnosis. *Adv Healthc Mater* 2020;9(9):1901058.
- [122] Colombo M, Carregal-Romero S, Casula MF, Gutiérrez L, Morales MP, Böhm IB, et al. Biological applications of magnetic nanoparticles. *Chem Soc Rev* 2012;41(11):4306–34.
- [123] Kandasamy G, Maity D. Recent advances in superparamagnetic iron oxide nanoparticles (SPIONs) for *in vitro* and *in vivo* cancer nanotheranostics. *Int J Pharm* 2015;496(2):191–218.
- [124] Wang J, Zhao K, Shen X, Zhang W, Ji S, Song Y, et al. Microfluidic synthesis of ultra-small magnetic nanohybrids for enhanced magnetic resonance imaging. *J Mater Chem C* 2015;3(48):12418–29.
- [125] Rezaian AH, Mousavi M, Kheirjou S, Amoabediny G, Ardestani MS, Mohammadnejad J. Monodisperse magnetite (Fe<sub>3</sub>O<sub>4</sub>) nanoparticles modified with water soluble polymers for the diagnosis of breast cancer by MRI method. *J Magn Mater* 2016;420:210–17.
- [126] Anbarasu M, Anandan M, Chinnasamy E, Gopinath V, Balamurugan K. Synthesis and characterization of polyethylene glycol (PEG) coated Fe<sub>3</sub>O<sub>4</sub> nanoparticles by chemical co-precipitation method for biomedical applications. *Spectrochim Acta A Mol and Biomol Spectrosc* 2015;135:536–9.
- [127] Fernández BI, Muñoz HM, Ruiz CJ, Herranz F, Pellico J. Iron oxide nanoparticles: an alternative for positive contrast in magnetic resonance imaging. *Inorganics* 2020;8(4):28.
- [128] Thomas R, Park IK, Jeong YY. Magnetic iron oxide nanoparticles for multimodal imaging and therapy of cancer. *Int J Mol Sci* 2013;14(8):15910–30.
- [129] Ferreira M, Sousa J, Pais A, Vitorino C. The role of magnetic nanoparticles in cancer nanotheranostics. *Materials (Basel)* 2020;13(2):266.
- [130] Shin TH, Choi Y, Kim S, Cheon J. Recent advances in magnetic nanoparticle-based multi-modal imaging. *Chem Soc Rev* 2015;44(14):4501–16.
- [131] Alphandéry E. Iron oxide nanoparticles as multimodal imaging tools. *RSC Adv* 2019;9(69):40577–87.
- [132] Meola A, Rao J, Chaudhary N, Song G, Zheng X, Chang SD. Magnetic particle imaging in neurosurgery. *World Neurosurg* 2019;125:261–70.
- [133] Tay ZW, Chandrasekharan P, Chiu-Lam A, Hensley DW, Dhavalikar R, Zhou XY, et al. Magnetic particle imaging-guided heating *in vivo* using gradient fields for arbitrary localization of magnetic hyperthermia therapy. *ACS Nano* 2018;12(4):3699–713.
- [134] Pillarisetti S, Uthaman S, Huh KM, Koh YS, Lee S, Park IK. Multimodal composite iron oxide nanoparticles for biomedical applications. *Tissue Eng Regen Med* 2019;16(5):451–65.
- [135] Lin Y, Zhang K, Zhang R, She Z, Tan R, Fan Y, et al. Magnetic nanoparticles applied in targeted therapy and magnetic resonance imaging: crucial preparation parameters, indispensable pre-treatments, updated research advancements and future perspectives. *J Mater Chem B* 2020;8(28):5973–91.
- [136] Cai W, Gao T, Hong H, Sun J. Applications of gold nanoparticles in cancer nanotechnology. *Nanotechnol Sci Appl* 2008;1:17–32.
- [137] Kim G, Huang SW, Day KC, O'Donnell M, Agayan RR, Day MA, et al. Indocyanine-green-embedded PEBBLES as a contrast agent for photoacoustic imaging. *J Biomed Opt* 2007;12(4):044020.
- [138] Shashkov EV, Everts M, Galanzha EI, Zharov VP. Quantum dots as multimodal photoacoustic and photothermal contrast agents. *Nano Lett* 2008;8(11):3953–8.
- [139] De La Zerda A, Zavaleta C, Keren S, Vaithilingam S, Bodapati S, Liu Z, et al. Carbon nanotubes as photoacoustic molecular imaging agents in living mice. *Nat Nanotechnol* 2008;3(9):557–62.
- [140] Bae KH, Kim YB, Lee Y, Hwang J, Park H, Park TG. Bioinspired synthesis and characterization of gadolinium-labeled magnetite nanoparticles for dual contrast T<sub>1</sub>- and T<sub>2</sub>-weighted magnetic resonance imaging. *Bioconjug Chem* 2010;21(3):505–12.
- [141] Zhou Z, Huang D, Bao J, Chen Q, Liu G, Chen Z, et al. A synergistically enhanced T<sub>1</sub>-T<sub>2</sub> dual-modal contrast agent. *Adv Mater* 2012;24(46):6223–8.
- [142] Shin TH, Choi JS, Yun S, Kim IS, Song HT, Kim Y, et al. T<sub>1</sub> and T<sub>2</sub> dual-mode MRI contrast agent for enhancing accuracy by engineered nanomaterials. *ACS Nano* 2014;8(4):3393–401.
- [143] Li J, You J, Wu C, Dai Y, Shi M, Dong L, et al. T<sub>1</sub>-T<sub>2</sub> molecular magnetic resonance imaging of renal carcinoma cells based on nano-contrast agents. *Int J Nanomed* 2018;13:4607–25.
- [144] Bai C, Hu P, Liu N, Feng G, Liu D, Chen Y, et al. Synthesis of ultrasmall Fe<sub>3</sub>O<sub>4</sub> nanoparticles as T<sub>1</sub>-T<sub>2</sub> dual-modal magnetic resonance imaging contrast agents in rabbit hepatic tumors. *ACS Appl Nano Mater* 2020;3(4):3585–95.
- [145] Wang G, Zhang X, Liu Y, Hu Z, Mei X, Uvdal K. Magneto-fluorescent nanoparticles with high-intensity NIR emission, T<sub>1</sub>- and T<sub>2</sub>-weighted MR for multimodal specific tumor imaging. *J Mater Chem B* 2015;3(15):3072–80.
- [146] Zhang L, Tong S, Zhang Q, Bao G. Lipid-encapsulated Fe<sub>3</sub>O<sub>4</sub> nanoparticles for multimodal magnetic resonance/fluorescence imaging. *ACS Appl Nano Mater* 2020;3(7):6785–97.
- [147] Choi JS, Park JC, Nah H, Woo S, Oh J, Kim KM, et al. A hybrid nanoparticle probe for dual-modality positron emission tomography and magnetic resonance imaging. *Angew Chem Int Ed Engl* 2008;47(33):6259–62.
- [148] Forte E, Fiorenza D, Torino E, Costagliola di Polidoro A, Cavaliere C, Netti PA, et al. Radiolabeled PET/MRI nanoparticles for tumor imaging. *J Clin Med* 2019;9(1):89.
- [149] Sandiford L, Phinikaridou A, Protti A, Meszaros LK, Cui X, Yan Y, et al. Bisphosphonate-anchored pegylation and radiolabeling of superparamagnetic iron oxide:



- long-circulating nanoparticles for *in vivo* multimodal ( $T_1$  MRI-SPECT) imaging. *ACS Nano* 2013;7(1):500–12.
- [150] Wang P, Sun W, Guo J, Zhang K, Liu Y, Jiang Q, et al. One pot synthesis of zwitterionic 99 MTC doped ultrasmall iron oxide nanoparticles for SPECT/ $T_1$ -weighted MR dual-modality tumor imaging. *Colloids Surf B Biointerfaces* 2021;197:111403.
- [151] Hu Y, Yang J, Wei P, Li J, Ding L, Zhang G, et al. Facile synthesis of hyaluronic acid-modified  $Fe_3O_4/Au$  composite nanoparticles for targeted dual mode MR/CT imaging of tumors. *J Mater Chem B* 2015;3(47):9098–108.
- [152] Zhao HY, Liu S, He J, Pan CC, Li H, Zhou ZY, et al. Synthesis and application of strawberry-like  $Fe_3O_4$ -Au nanoparticles as CT-MR dual-modality contrast agents in accurate detection of the progressive liver disease. *Biomaterials* 2015;51:194–207.
- [153] Park JI, Jagadeesan D, Williams R, Oakden W, Chung S, Stanisiz GJ, Kumacheva E. Microbubbles loaded with nanoparticles: a route to multiple imaging modalities. *ACS Nano* 2010;4(11):6579–86.
- [154] Yang P, Luo X, Wang S, Wang F, Tang C, Wang C. Biodegradable yolk-shell microspheres for ultrasound/MR dual-modality imaging and controlled drug delivery. *Colloids Surf B Biointerfaces* 2017;151:333–43.
- [155] Mai X, Chang Y, You Y, He L, Chen T. Designing intelligent nano-bomb with on-demand site-specific drug burst release to synergize with high-intensity focused ultrasound cancer ablation. *J Control Rel* 2021;331:270–81.
- [156] Park S, Jung U, Lee S, Lee D, Kim C. Contrast-enhanced dual mode imaging: photoacoustic imaging plus more. *Biomed Eng Lett* 2017;7(2):121–33.
- [157] Ding N, Sano K, Kanazaki K, Shimizu Y, Watanabe H, Namita T, et al. Sensitive photoacoustic/magnetic resonance dual imaging probe for detection of malignant tumors. *J Pharm Sci* 2020;109(10):3153–9.
- [158] Yan C, Liu D, An L, Wang Y, Tian Q, Lin J, et al. Magnetic-photoacoustic dual-mode probe for the visualization of  $H_2S$  in colorectal cancer. *Anal Chem* 2020;92(12):8254–61.
- [159] Malhotra N, Lee JS, Liman RAD, Ruallo JMS, Villaflores OB, Ger TR, et al. Potential toxicity of iron oxide magnetic nanoparticles: a review. *Molecules (Basel)* 2020;25(14):3159.
- [160] Kim JE, Shin JY, Cho MH. Magnetic nanoparticles: an update of application for drug delivery and possible toxic effects. *Arch Toxicol* 2012;86(5):685–700.
- [161] Cole AJ, Yang VC, David AE. Cancer theranostics: the rise of targeted magnetic nanoparticles. *Trends Biotechnol* 2011;29(7):323–32.
- [162] Alphandéry E. Biodistribution and targeting properties of iron oxide nanoparticles for treatments of cancer and iron anemia disease. *Nanotoxicology* 2019;13(5):573–96.
- [163] Jain TK, Reddy MK, Morales MA, Leslie-Pelecky DL, Labhasetwar V. Biodistribution, clearance, and biocompatibility of iron oxide magnetic nanoparticles in rats. *Mol Pharm* 2008;5(2):316–27.
- [164] Chertok B, David AE, Yang VC. Polyethyleneimine-modified iron oxide nanoparticles for brain tumor drug delivery using magnetic targeting and intra-carotid administration. *Biomaterials* 2010;31(24):6317–24.
- [165] Sakulku U, Mahmoudi M, Maurizi L, Salaklang J, Hofmann H. Protein corona composition of superparamagnetic iron oxide nanoparticles with various physico-chemical properties and coatings. *Sci Rep* 2014;4(1):5020.
- [166] Huang J, Bu L, Xie J, Chen K, Cheng Z, Li X, et al. Effects of nanoparticle size on cellular uptake and liver MRI with polyvinylpyrrolidone-coated iron oxide nanoparticles. *ACS Nano* 2010;4(12):7151–60.
- [167] Levy M, Luciani N, Alloyeau D, Elgrabli D, Deveaux V, Pechoux C, et al. Long term *in vivo* biotransformation of iron oxide nanoparticles. *Biomaterials* 2011;32(16):3988–99.
- [168] El-Sherbiny IM, Elbaz NM, Sedki M, Elgammal A, Yacoub MH. Magnetic nanoparticles-based drug and gene delivery systems for the treatment of pulmonary diseases. *Nanomedicine (Lond)* 2017;12(4):387–402.
- [169] Martin AR, Thompson RB, Finlay WH. MRI measurement of regional lung deposition in mice exposed nose-only to nebulized superparamagnetic iron oxide nanoparticles. *J Aerosol Med Pulm Drug Deliv* 2008;21(4):335–42.
- [170] Kawish M, Elhissi A, Jabri T, Iqbal KM, Zahid H, Shah MR. Enhancement in oral absorption of ceftriaxone by highly functionalized magnetic iron oxide nanoparticles. *Pharmaceutics* 2020;12(6):492.
- [171] Kaliyamoorthi K, Sumohan Pillai A, Alexander A, Ramasamy S, Arivarasu A, Enoch IVMV. Designed poly(ethylene glycol) conjugate-erbium-doped magnetic nanoparticle hybrid carrier: enhanced activity of anticancer drug. *J Mater Sci* 2021;56(5):3925–34.
- [172] Próspero AG, Quini CC, Bakuzis AF, Fidelis-de-Oliveira P, Moretto GM, Mello PPF, et al. Real-time *in vivo* monitoring of magnetic nanoparticles in the bloodstream by AC biosusceptometry. *J Nanobiotechnol* 2017;15(1):22.
- [173] Sandler SE, Fellows B, Mefford OT. Best practices for characterization of magnetic nanoparticles for biomedical applications. *Anal Chem* 2019;91(22):14159–69.
- [174] Ferreira M, Sousa J, Pais A, Vitorino C. The role of magnetic nanoparticles in cancer nanotheranostics. *Materials (Basel)* 2020;13(2):266.
- [175] Giustini AJ, Ivkov R, Hoopes PJ. Magnetic nanoparticle biodistribution following intratumoral administration. *Nanotechnology* 2011;22(34):345101.
- [176] Vakili-Ghartavol R, Momtazi-Borojeni AA, Vakili-Ghartavol Z, Aiyelabegan HT, Jaafari MR, Rezayat SM, et al. Toxicity assessment of superparamagnetic iron oxide nanoparticles in different tissues. *Artif Cells Nanomed Biotechnol* 2020;48(1):443–51.
- [177] Nosrati H, Salehiabar M, Fridoni M, Abdollahifar MA, Kheiri Manjili H, Davaran S, et al. New insight about biocompatibility and biodegradability of iron oxide magnetic nanoparticles: stereological and *in vivo* MRI monitor. *Sci Rep* 2019;9(1):7173.
- [178] Wang L, Wang Z, Li X, Zhang Y, Yin M, Li J, et al. Deciphering active biocompatibility of iron oxide nanoparticles from their intrinsic antagonism. *Nano Res* 2018;11(5):2746–55.
- [179] Tiwary GS, Mudakavi RJ, Kishore S, Kashyap S, Elumalai R, Chakravorty D, et al. Magnetic iron nanoparticles for *in vivo* targeted delivery and as biocompatible contrast agents. *RSC Adv* 2016;6(115):114344–52.
- [180] Frtús A, Smolková B, Uzhytchak M, Lunova M, Jirsa M, Kubinová Š, et al. Analyzing the mechanisms of iron oxide nanoparticles interactions with cells: a road from failure to success in clinical applications. *J Control Rel* 2020;328:59–77.
- [181] Patil US, Adireddy S, Jaiswal A, Mandava S, Lee BR, Chrisey DB. *In vitro/in vivo* toxicity evaluation and quantification of iron oxide nanoparticles. *Int J Mol Sci* 2015;16(10):24417–50.
- [182] Yarjanli Z, Ghaedi K, Esmaeili A, Rahgozar S, Zarrabi A. Iron oxide nanoparticles may damage to the neural tissue through iron accumulation, oxidative stress, and protein aggregation. *BMC Neurosci* 2017;18(1):51.
- [183] Ying E, Hwang HM. *In vitro* evaluation of the cytotoxicity of iron oxide nanoparticles with different coatings and different sizes in  $A_3$  human T lymphocytes. *Sci Total Environ* 2010;408(20):4475–81.
- [184] Sukhanova A, Bozrova S, Sokolov P, Berestovoy M, Karaulov A, Nabiev I. Dependence of nanoparticle toxicity

- on their physical and chemical properties. *Nanoscale Res Lett* 2018;13(1):44.
- [185] Karlsson HL, Gustafsson J, Cronholm P, Möller L. Size-dependent toxicity of metal oxide particles—a comparison between nano- and micrometer size. *Toxicol Lett* 2009;188(2):112–18.
- [186] Lee JH, Ju JE, Kim BI, Pak PJ, Choi EK, Lee HS, et al. Rod-shaped iron oxide nanoparticles are more toxic than sphere-shaped nanoparticles to murine macrophage cells. *Environ Toxicol Chem* 2014;33(12):2759–66.
- [187] Kumar V, Sharma N, Maitra SS. *In vitro* and *in vivo* toxicity assessment of nanoparticles. *Int Nano Lett* 2017;7(4):243–56.
- [188] Fahmy HM, Aly EM, Mohamed FF, Noor NA, Elsayed AA. Neurotoxicity of green-synthesized magnetic iron oxide nanoparticles in different brain areas of wistar rats. *Neurotoxicology* 2020;77:80–93.
- [189] Zhu X, Tian S, Cai Z. Toxicity assessment of iron oxide nanoparticles in zebrafish (*Danio rerio*) early life stages. *PLoS One* 2012;7(9):e46286.
- [190] Cristea C, Tertis M, Galatus R. Magnetic nanoparticles for antibiotics detection. *Nanomaterials (Basel)* 2017;7(6):119.
- [191] Xu JK, Zhang FF, Sun JJ, Sheng J, Wang F, Sun M. Bio and nanomaterials based on Fe<sub>3</sub>O<sub>4</sub>. *Molecules* 2014;19(12):21506–28.
- [192] Hyeon T. Chemical synthesis of magnetic nanoparticles. *Chem Commun (Camb)* 2003(8):927–34.
- [193] Jiang H, Wu H, Xu YL, Wang JZ, Zeng Y. Preparation of galactosylated chitosan/tripolyphosphate nanoparticles and application as a gene carrier for targeting SMMC<sub>7721</sub> cells. *J Biosci and Bioeng* 2011;111(6):719–24.
- [194] Jin D, Jiang X, Jing X, Ou Z. Effects of concentration, head group, and structure of surfactants on the degradation of phenanthrene. *J Hazard Mater* 2007;144(1):215–21.
- [195] Wallyn J, Anton N, Akram S, Vandamme TF. Biomedical imaging: principles, technologies, clinical aspects, contrast agents, limitations and future trends in nanomedicines. *Pharm Res* 2019;36(6):78.
- [196] Shen S, Wang S, Zheng R, Zhu X, Jiang X, Fu D, Yang W. Magnetic nanoparticle clusters for photothermal therapy with near-infrared irradiation. *Biomaterials* 2015;39:67–74.
- [197] Ran Q, Xiang Y, Liu Y, Xiang L, Li F, Deng X, et al. Eryptosis indices as a novel predictive parameter for biocompatibility of Fe<sub>3</sub>O<sub>4</sub> magnetic nanoparticles on erythrocytes. *Sci Rep* 2015;5(1):16209.
- [198] Correia Carreira S, Walker L, Paul K, Saunders M. The toxicity, transport and uptake of nanoparticles in the *in vitro* BeWo b30 placental cell barrier model used within NanoTEST. *Nanotoxicology* 2015;9(1):66–78.
- [199] Shukla S, Jadaun A, Arora V, Sinha RK, Biyani N, Jain VK. *In vitro* toxicity assessment of chitosan oligosaccharide coated iron oxide nanoparticles. *Toxicol Rep* 2014;2:27–39.
- [200] Gholami A, Rasoul AS, Ebrahiminezhad A, Seradj SH, Ghasemi Y. Lipoamino acid coated superparamagnetic iron oxide nanoparticles concentration and time dependently enhanced growth of human hepatocarcinoma cell line (Hep-G2). *J Nanomater* 2015;2015:451405.
- [201] Marcus M, Karni M, Baranes K, Levy I, Alon N, Margel S, Shefi O. Iron oxide nanoparticles for neuronal cell applications: uptake study and magnetic manipulations. *J Nanobiotechnol* 2016;14(1):37.
- [202] Nosrati H, Salehiabar M, Attari E, Davaran S, Danafar H, Manjili HK. Green and one-pot surface coating of iron oxide magnetic nanoparticles with natural amino acids and biocompatibility investigation. *Appl Organomet Chem* 2018;32(2):e4069.
- [203] Shevtsov M, Nikolaev B, Marchenko Y, Yakovleva L, Skvortsov N, Mazur A, et al. Targeting experimental orthotopic glioblastoma with chitosan-based superparamagnetic iron oxide nanoparticles (CS-DX-SPIONs). *Int J Nanomed* 2018;13:1471–82.
- [204] Chandekar KV, Shkir M, Alshahrani T, Ibrahim EH, Kilany M, Ahmad Z, et al. One-spot fabrication and *in-vivo* toxicity evaluation of core-shell magnetic nanoparticles. *Mater Sci Eng C* 2021;122:111898.
- [205] Ahmad A, Ansari MM, Kumar A, Vyawahare A, Mishra RK, Jayamurugan G, et al. Comparative acute intravenous toxicity study of triple polymer-layered magnetic nanoparticles with bare magnetic nanoparticles in swiss albino mice. *Nanotoxicology* 2020;14(10):1362–80.
- [206] Malhotra N, Chen JR, Sarasamma S, Audira G, Siregar P, Liang ST, et al. Ecotoxicity assessment of Fe<sub>3</sub>O<sub>4</sub> magnetic nanoparticle exposure in adult zebrafish at an environmental pertinent concentration by behavioral and biochemical testing. *Nanomaterials (Basel)* 2019;9(6):873.
- [207] Di Bona KR, Xu Y, Gray M, Fair D, Hayles H, Milad L, et al. Short- and long-term effects of prenatal exposure to iron oxide nanoparticles: influence of surface charge and dose on developmental and reproductive toxicity. *Int J Mol Sci* 2015;16(12):30251–68.
- [208] Saatchi K, Tod SE, Leung D, Nicholson KE, Andreu I, Buchwalder C, et al. Characterization of alendronic- and undecylenic acid coated magnetic nanoparticles for the targeted delivery of rosiglitazone to subcutaneous adipose tissue. *Nanomedicine* 2017;13(2):559–68.
- [209] Feng Q, Liu Y, Huang J, Chen K, Huang J, Xiao K. Uptake, distribution, clearance, and toxicity of iron oxide nanoparticles with different sizes and coatings. *Sci Rep* 2018;8(1):2082.
- [210] Caro C, Egea-Benavente D, Polvillo R, Royo JL, Pernia LM, García-Martín ML. Comprehensive toxicity assessment of PEGylated magnetic nanoparticles for *in vivo* applications. *Colloids Surf B Biointerfaces* 2019;177:253–9.
- [211] Salimi M, Sarkar S, Fathi S, Alizadeh AM, Saber R, Moradi F. Biodistribution, pharmacokinetics, and toxicity of dendrimer-coated iron oxide nanoparticles in BALB/c mice. *Int J Nanomed* 2018;13:1483–93.